Eur. Phys. J. C (2019) 79:803
https://doi.org/10.1140/epjc/s10052-019-7295-1

THE EUROPEAN PHYSICAL JOURNAL C

Regular Article - Experimental Physics

Search for excited electrons singly produced in proton–proton collisions at $\sqrt{s} = 13$ TeV with the ATLAS experiment at the LHC

ATLAS Collaboration[⋆]

CERN, 1211 Geneva 23, Switzerland

Received: 11 June 2019 / Accepted: 11 September 2019 / Published online: 26 September 2019

Abstract A search for excited electrons produced in pp collisions at $\sqrt{s} = 13$ TeV via a contact interaction $q\bar{q} \to ee^*$ is presented. The search uses 36.1 fb^{-1} of data collected in 2015 and 2016 by the ATLAS experiment at the Large Hadron Collider. Decays of the excited electron into an electron and a pair of quarks ($eq\bar{q}$) are targeted in final states with two electrons and two hadronic jets, and decays via a gauge interaction into a neutrino and a W boson (νW) are probed in final states with an electron, missing transverse momentum, and a large-radius jet consistent with a hadronically decaying W boson. No significant excess is observed over the expected backgrounds. Upper limits are calculated for the $pp \to ee^* \to eeq\bar{q}$ and $pp \to ee^* \to e\nu W$ production cross sections as a function of the excited electron mass m_{e^*} at 95% confidence level. The limits are translated into lower bounds on the compositeness scale parameter Λ of the model as a function of m_{e^*}. For $m_{e^*} < 0.5$ TeV, the lower bound for Λ is 11 TeV. In the special case of $m_{e^*} = \Lambda$, the values of $m_{e^*} < 4.8$ TeV are excluded. The presented limits on Λ are more stringent than those obtained in previous searches.

1 Introduction

Excited leptons appear in a number of composite models [1–6] seeking to explain the existence of the three generations of quarks and leptons in the Standard Model (SM). This analysis uses the model presented in Ref. [6] as a benchmark. The composite models introduce new constituent particles called preons that bind at a high scale Λ to form SM fermions and their excited states. The preon bound states are mapped into representations of the $SU(2) \times U(1)$ SM gauge group. The SM fermions are identified as a set of left- and right-handed chiral states protected by the $SU(2)$ symmetry from obtaining masses of the order of Λ [6]. The remaining vector-like states, $SU(2)$ doublets and singlets, acquire masses of the order of Λ and are thus interpreted as excited fermions.

⋆ e-mail: atlas.publications@cern.ch

The effective Lagrangian introduces four-fermion contact-interaction (CI) terms (Eqs. (1) and (2)) and gauge-mediated (GM) currents (Eq. (3)):

$$\Delta\mathcal{L}_{\mathrm{CI}} = \frac{2\pi}{\Lambda^2} j^\mu j_\mu \tag{1}$$

$$j_\mu = \bar{f}_{\mathrm{L}}\gamma_\mu f_{\mathrm{L}} + \bar{f}^*_{\mathrm{L}}\gamma_\mu f^*_{\mathrm{L}} + \left(\bar{f}^*_{\mathrm{L}}\gamma_\mu f_{\mathrm{L}} + \mathrm{H.C.}\right) \tag{2}$$

$$\Delta\mathcal{L}_{\mathrm{GM}} = \frac{1}{2\Lambda}\bar{f}^*_{\mathrm{R}}\sigma^{\mu\nu}\left[g\frac{\tau}{2}W_{\mu\nu} + g'\frac{Y}{2}B_{\mu\nu}\right] f_{\mathrm{L}} + \mathrm{H.C.} \tag{3}$$

Here, $f = \ell, q$ and $f^* = \ell^*, q^*$ denote SM and excited leptons and quarks, and the subscripts L and R stand for left- and right-handed components of the fermion field f, respectively. The j_μ term is the fermion current of f and f^*. The $W_{\mu\nu}$ and $B_{\mu\nu}$ are the field-strength tensors of the $SU(2)$ and $U(1)$ gauge fields, and g and g' are the corresponding coupling constants of the electroweak theory. The left- and right-handed excited fermions are both $SU(2)$ doublets, with the weak hypercharge Y such that f^* electric charges coincide with the ones of their ground states f. The weak hypercharge Y of the $\ell^*_{\mathrm{L,R}}$ doublet is -1, so that its isospin $T_3 = -1/2$ component represents an excited lepton with electric charge $Q = -1$. Therefore, the excited lepton model introduces two unknown parameters relevant for this analysis, the excited lepton mass m_{e^*} and the compositeness scale Λ, which define the preferred search channels and kinematic properties of the final states. The four-fermion CI terms are suppressed by $1/\Lambda^2$ implying the parton-level e^* production cross section growing proportionally to $\hat{s}$. The considered models allow only left-handed currents in the contact-interaction terms, and all dimensionless couplings defining the relative strength of the residual interactions are set to unity [6]. The restriction $m_{e^*} < \Lambda$ follows from unitarity constraints on the contact interactions [6,7]. Branching ratios ($\mathcal{B}$) for excited electrons as functions of m_{e^*} for the case of $\Lambda = 10$ TeVare presented in Fig. 1. Gauge-mediated decays dominate at $m_{e^*} \ll \Lambda$ while the decay via a contact interaction becomes dominant for $m_{e^*} \gtrsim \Lambda/3$.

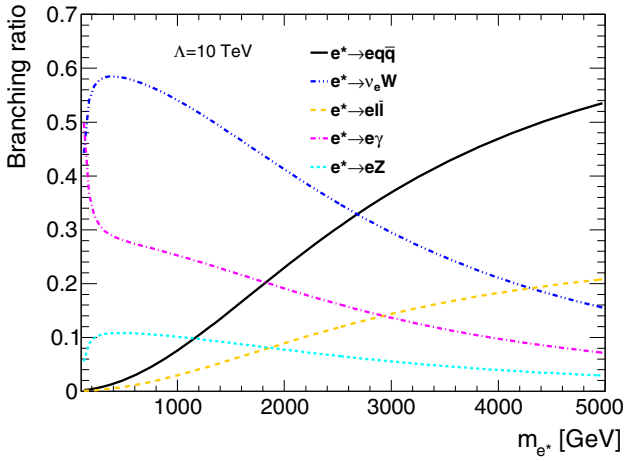

Fig. 1 Branching ratios for excited electrons as a function of m_{e^*}. The scale Λ is set to 10 TeV

This article presents a search for excited electrons singly produced in pp collisions at $\sqrt{s} = 13$ TeV via a contact interaction $q\bar{q} \rightarrow ee^*$ and decaying either to an electron and a pair of quarks ($eq\bar{q}$) via a contact interaction or to a neutrino and a W boson (νW) via a gauge interaction, depicted in Fig. 2a, b, respectively. Given the sensitivity of the search, the contribution of gauge-mediated production of the excited electrons is non-negligible relative to the contact-interaction production only for $m_{e^*} < 200$ GeV [8] and thus neglected. The search uses 36.1 fb^{-1} of data collected in 2015 and 2016 by the ATLAS experiment [9] at the Large Hadron Collider (LHC).

The present search uses two experimental channels. The first channel targets the production of excited electrons via a contact interaction $q\bar{q} \rightarrow ee^*$ and their decay via a contact interaction $e^* \rightarrow eq\bar{q}$, resulting in two energetic electrons and at least two hadronic jets j. In the second channel, the excited electrons are produced via a contact interaction as well, but their decay is via a gauge-mediated interaction into a W and a ν, where the W boson decays hadronically, yielding an $ee^* \rightarrow e\nu q\bar{q}$ final state. Experimentally, this gives final states with exactly one energetic electron, a large-radius (large-R) jet J produced by two collimated quarks, and missing transverse momentum. The large-R jet approach is sufficient for the current analysis, as the analysis selection with two resolved jets has minor efficiency. In the following, the final states resulting from contact- and gauge-mediated decays of singly produced e^* are denoted by $eejj$ and $e\nu J$, respectively. The combination of the two channels maximizes the sensitivity of the search for all m_{e^*}/Λ values. For possible reinterpretations, the results are also presented in terms of model-independent upper limits on the number of signal events and on the visible signal cross section.

Previous searches for excited leptons were carried out at LEP [10–13], HERA [14,15], the Tevatron [16–19], and the LHC [8,20–26]. No evidence of excited leptons was found and bounds were set on m_{e^*}, which is limited to be greater than 3 TeV for the compositeness scale $\Lambda = m_{e^*}$ [21].

2 ATLAS detector

The ATLAS detector [9] is a multipurpose detector with a forward–backward symmetric cylindrical geometry and nearly 4π coverage in solid angle.[1] The three major subcomponents of ATLAS are the tracking detector, the calorimeter, and the muon spectrometer. Charged-particle tracks and vertices are reconstructed by the inner detector (ID) tracking system, comprising silicon pixel (including the newly installed innermost pixel layer [27,28]) and silicon microstrip detectors covering the pseudorapidity range $|\eta| < 2.5$, and a straw-tube tracker that covers $|\eta| < 2.0$. The ID is immersed in a homogeneous 2 T magnetic field provided by a solenoid. The energies of electrons, photons, and jets are measured with sampling calorimeters. The ATLAS calorimeter system covers a pseudorapidity range of $|\eta| < 4.9$. Within the region $|\eta| < 3.2$, electromagnetic (EM) calorimetry is performed with barrel and endcap high-granularity lead/liquid argon (LAr) calorimeters, with an additional thin LAr presampler covering $|\eta| < 1.8$ to correct for energy loss in material upstream of the calorimeters. Hadronic calorimetry is performed with a steel/scintillator-tile calorimeter, segmented into three barrel structures within $|\eta| < 1.7$, and two copper/LAr endcap calorimeters. The forward region ($3.1 < |\eta| < 4.9$) is instrumented with a LAr calorimeter with copper and tungsten absorbers for EM and hadronic energy measurements, respectively. Surrounding the calorimeters is a muon spectrometer (MS) with superconducting air-core toroidal magnets. The field integral of the toroids ranges between 2.0 and 6.0 T m across most of the detector. The MS includes three stations of precision tracking chambers covering $|\eta| < 2.7$ to measure the curvature of tracks. The MS also contains detectors with triggering capabilities covering $|\eta| < 2.4$ to provide fast muon identification and momentum measurements.

The ATLAS two-level trigger system selects events as described in Ref. [29]. The first-level trigger is hardware-based while the second, high-level trigger is implemented in software and employs algorithms similar to those used offline in the full event reconstruction.

[1] ATLAS uses a right-handed coordinate system with its origin at the nominal interaction point (IP) in the centre of the detector and the z-axis along the beam pipe. The x-axis points from the IP to the centre of the LHC ring, and the y-axis points upward. Cylindrical coordinates (r, ϕ) are used in the transverse plane, ϕ being the azimuthal angle around the z-axis. The pseudorapidity is defined in terms of the polar angle θ as $\eta = -\ln\tan(\theta/2)$. Angular distance is measured in units of $\Delta R \equiv \sqrt{(\Delta\eta)^2 + (\Delta\phi)^2}$.

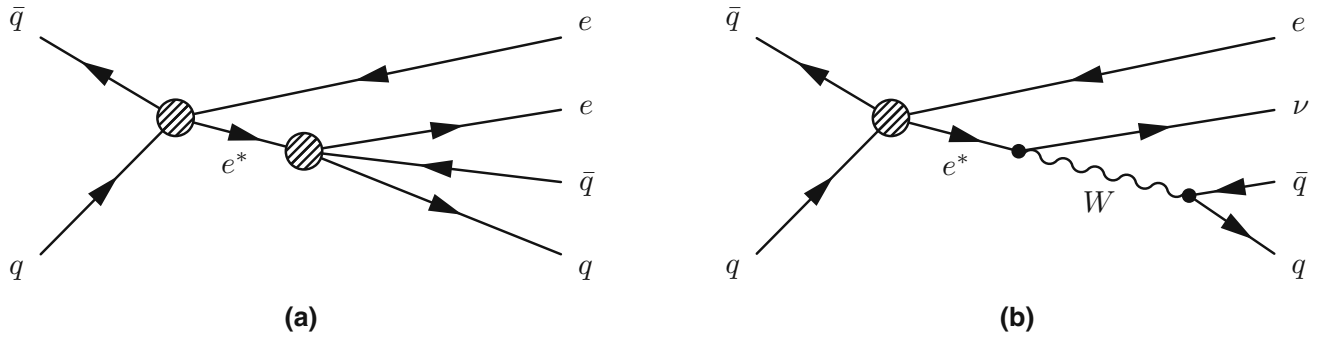

Fig. 2 Feynman diagrams for **a** $ee^* \to eeq\bar{q}$ and **b** $ee^* \to e\nu W$

3 Data and simulated event samples

The analysis uses the pp collision data recorded by the ATLAS detector in 2015 and 2016 at $\sqrt{s}$ = 13 TeV with a 25 ns bunch spacing. The total integrated luminosity collected in the data-taking periods with normal operation of the relevant detector subsystems is 36.1 fb^{-1}. To further improve the data quality, events containing noise bursts or coherent noise in the calorimeters, as well as incompletely recorded events, are excluded.

Events for the $eejj$ channel were recorded using dielectron triggers with transverse energy E_{T} thresholds of 12 and 17 GeV for both electrons in 2015 and 2016, respectively. For the $e\nu J$ channel, events must pass at least one of the two single-electron trigger requirements with thresholds set at E_{T} = 60 or 120 GeV in 2015, and E_{T} = 60 or 140 GeV in 2016. Combining the lower-threshold trigger with the one with a higher threshold but looser identification requirements, results in single-electron trigger efficiencies typically exceeding 90% for the electrons in the phase space considered in the analysis [29]. Events with an $e\mu jj$ final state are used for background studies in the $eejj$ channel and are selected using a combination of the two single-muon triggers with the transverse momentum p_{T} thresholds of 26 and 50 GeV.

Selected events contain proton–proton collisions in the same or neighboring bunch crossing (pile-up). The events used in the analysis contain 24 pile-up interactions on average, resulting in multiple interaction vertices in an event. The primary vertex (PV) is defined as the vertex with the highest Σp_{T}^2 of charged-particle tracks. This PV must have at least two tracks with the transverse momentum $p_{\mathrm{T}} > 400$ MeV.

The signal samples were simulated by Pythia 8.210 [30], using a leading-order (LO) matrix element (ME), the NNPDF23LO [31] set of parton distribution functions (PDFs) and the A14 [32] set of tuned parameters. The e^* widths for the simulated signal samples were derived from CalcHEP 3.6.25 [33], which takes into account phase-space effects due to quark masses. The samples were generated for a compositeness scale Λ = 5 TeV and masses of excited electrons ranging from 100 GeV to 4 TeV. The effect of a finite Λ-dependent e^* width on the analysis is negligible for $m_{e^*} < \Lambda$.

As shown in Sect. 5, the dominant backgrounds in the $eejj$ and $e\nu J$ channels are from $Z/\gamma^* +$ jets and $W +$ jets production, respectively. The sub-leading background in both channels is from $t\bar{t}$ production, followed by single-top and diboson production. The estimation of background processes involving prompt leptons from W and Z/γ^* decays relies on simulated event samples.

The $Z/\gamma^* +$ jets and $W +$ jets processes were simulated using Sherpa 2.2.1 [34]. Parton-level final states with up to two partons produced along with the Z and W bosons were generated at next-to-leading order (NLO), and those with three or four partons were generated at LO, using the OpenLoops [35] and Comix [36] for the NLO and LO cases, respectively. Double counting of events with the same partonic final state generated by various combinations of the ME and parton shower (PS) was eliminated according to the ME+PS@NLO prescription [37]. The NNPDF 3.0 [38] set of PDFs was used. The $Z/\gamma^* +$ jets and $W +$ jets simulated event samples were normalized to the next-to-next-to-leading-order (NNLO) inclusive cross sections computed with the FEWZ program [39].

The $t\bar{t}$ simulated event samples were generated at NLO accuracy in the strong coupling constant using Powheg-Box v2 [40–43], with the top-quark spin correlations preserved, and the CT10 [44] PDF set. Electroweak s- and t-channel single-top-quark events as well as events with a single top-quark produced in association with a W boson were generated using Powheg- Box v1 [45,46]. Parton showering, hadronization and the underlying event were handled by Pythia 8.210 for $t\bar{t}$ production and by Pythia 6.428 [47] for single-top production. Pythia 8.210 and Pythia 6.428 used the A14 and Perugia 2012 [48] sets of tuned parameters, respectively. The $t\bar{t}$ simulated event sample was normalized to the inclusive cross section calculated using the Top++ v2.0 [49] at NNLO accuracy in the strong

Table 1 Object definitions in the $eejj$ and $e\nu J$ channels. Muon selections are given in parentheses

Selection type	Objects	$eejj$	$e\nu J$
Baseline	Electrons (muons)	$p_{\mathrm{T}} > 30$ GeV (> 40 GeV)	$p_{\mathrm{T}} > 40$ GeV
		$\lvert\eta\rvert < 2.47$, excluding $1.37 < \lvert\eta\rvert < 1.52$ (< 2.5)	
		Both channels: Quality *loose* (*medium*)	
		Both channels: No isolation (*loose* isolation with ID tracks)	
		$\lvert d_0\rvert/\sigma_{d_0} < 5$ (< 3); $\lvert z_0 \sin\theta\rvert < 0.5$ mm	
	Jets	*Both channels*: $R = 0.4$ jets, $p_{\mathrm{T}} > 20$ GeV	
	b-jets	–	$R = 0.4$ jets
			$\lvert\eta\rvert < 2.5$, JVT
Final	Electrons	$p_{\mathrm{T}} > 30$ GeV	$p_{\mathrm{T}} > 65$ GeV
		Quality *medium*	Quality *tight*
		Both channels: *Loose* isolation	
	Jets	$R = 0.4$ jets	$R = 1.0$ jets
		$p_{\mathrm{T}} > 50$ GeV	$p_{\mathrm{T}} > 200$ GeV
		$\lvert\eta\rvert < 2.8$, JVT	$\lvert\eta\rvert < 2$

coupling constant, with soft gluon emission accounted for in the next-to-next-to-leading logarithmic order (NNLL). The single-top simulated event samples were normalized to the cross sections computed at NLO+NNLL accuracy [50].

The ZZ, ZW and WW simulated event samples were generated using SHERPA 2.2.1. Events containing zero or one final-state parton were generated using an NLO ME. Events with two or three recoiling quarks or gluons were generated with a LO ME. The NNPDF 3.0 PDF set was used. The event generator cross sections are used in this case.

Decays of b- and c-hadrons in the simulated event samples of $t\bar{t}$, single-top, and signal processes were handled by EvtGen v1.2.0 [51].

The pile-up interactions are described by overlaying minimum-bias events on each simulated signal or background event. The minimum-bias events were generated with PYTHIA 8.186 [52] with the A2 [53] set of tuned parameters and the MSTW2008LO [54] PDFs. The distribution of the average number of interactions per bunch crossing in simulated event samples is reweighted to match the observed data.

All the simulated event samples were passed through a simulation of the ATLAS detector [55]. The detector response was obtained from a detector model that uses GEANT4 [56]. For the simulation of the $ee^* \rightarrow eeq\bar{q}$ signal samples, GEANT4 based inner detector simulation was combined with a parameterized calorimeter simulation [55]. The simulated event samples were processed with the same reconstruction software as used for data.

4 Object and event selection

Events satisfying basic quality, trigger and vertex requirements are selected for the analysis using the criteria applied to electrons, muons, hadronic jets, and their kinematic quantities. The looser *baseline* selections are applied at stages which aim to eliminate double counting of detected objects (electrons, muons, jets, tracks, vertices, etc.) in an event and double-counting of events in the two analysis channels. The tighter *final* selection defines objects used in the analysis. In the following, both the *baseline* and *final* object selections are specified in Table 1, and the order of the event criteria applied in the analysis is given in Table 2. These selections form the *preselection* stage.

An electron candidate is reconstructed as a clustered energy deposition in the calorimeter matched to a track from the ID [57]. The direction of an electron is taken from its track and the energy is measured from the EM cluster. The energy is corrected for losses in the material before the calorimeter and for leakage outside of the cluster [58]. The coverage of the ID limits the pseudorapidity of electrons to $\lvert\eta\rvert < 2.47$. Electrons with $1.37 < \lvert\eta\rvert < 1.52$ are excluded because they point to the barrel-to-endcap transition regions. To reject electron candidates originating from hadronic jets and photon conversions, electrons are required to satisfy a set of likelihood-based identification criteria determined by variables characterizing longitudinal and lateral calorimeter shower shapes, ID track properties, and track–cluster matching. These criteria are referred to, in order of increasing background rejection, as *loose*, *medium* and *tight* and are defined so that an electron satisfying a tighter criterion always satisfies looser ones. The *loose* identification is approximately 95% efficient for prompt electrons with $p_{\mathrm{T}} > 30$ GeV. In the same p_{T} range, signal efficiency for *medium* identifi-

Table 2 Event selection sequences in the $eejj$ and evJ channels. W-tag50 refers to the W-tagger with a 50% signal efficiency. 'Truth matching' requires selected electrons to match electrons from the event generators

	$eejj$	evJ
Overlap removal (1)	Between *baseline*	Between *baseline*
	Electrons, muons, jets	Electrons, muons, jets, b-jets
Jet cleaning	*Both channels*: Reject event if it has a *baseline* $R = 0.4$ jet of non-collision origin	
Overlap removal (2)	–	Between *baseline* electrons and *final* $R = 1.0$ jets
Number of jets	$N^{\text{jets}}_{\text{final}} \geq 2$	$N^{J}_{\text{final}} \geq 1$
Number of leptons	$N^{e}_{\text{final}} = 2$	$N^{e}_{\text{final}} = 1$
	$N^{e}_{\text{baseline}} \geq 2$ and $N^{\mu}_{\text{baseline}} = 0$	$N^{e}_{\text{baseline}} = 1$ and $N^{\mu}_{\text{baseline}} = 0$
Trigger matching	*Both channels*: Reject event if *final* electrons are not matched to the trigger objects	
Truth matching	*Both channels*: Simulation only: reject event if a selected electron fails truth matching	
$E_{\text{T}}^{\text{miss}}$	–	$E_{\text{T}}^{\text{miss}} > 100$ GeV
m_J		$m^{J}_{\text{final}} > 50$ GeV
$D_2^{\beta=1}$		Reject event if
		Final $R = 1.0$ jet does not satisfy
		Upper bound on $D_2^{\beta=1}$ for W-tag50

cation is greater than 90%. The efficiency of *tight* identification is greater than 85% for prompt electrons with $p_{\text{T}} >$ 65 GeV [57]. Further rejection of background is achieved by applying EM calorimeter and ID isolation requirements [57]. The *loose* isolation requirement applied in this analysis is designed to achieve 99% selection efficiency for prompt electrons. Electrons originating from the primary interaction vertex are selected by requiring the reconstructed electron track to have a transverse impact parameter significance $|d_0|/\sigma_{d_0} < 5$, where σ_{d_0} is the uncertainty in the transverse impact parameter, and a longitudinal impact parameter $|z_0 \sin\theta| < 0.5$ mm.

Muons are reconstructed using a combined fit of tracks measured with the ID and MS. Muons from in-flight decays of charged hadrons are suppressed with the *medium* set of identification requirements [59]. The muon identification efficiency exceeds 96% for prompt muons with $p_{\text{T}} > 20$ GeV. Muons are also subject to a *loose* isolation requirement that uses ID tracks [59] and is 99% efficient for prompt muons at any relevant p_{T} and η. Muons are further required to originate from the primary vertex by imposing the same criteria as for electrons on the ID track's longitudinal impact parameter and transverse impact parameter significance less then 3.

Hadronic jets are reconstructed from clustered energy deposits in the calorimeters using the anti-k_t algorithm [60] with radius parameters $R = 0.4$ and $R = 1.0$. The reconstructed jets with $R = 1.0$ are trimmed [61] to reduce contributions from pile-up interactions and underlying event by reclustering the jet constituents into subjets using a k_t algorithm with $R = 0.2$ and removing subjets carrying less than 5% of the boosted jet's p_{T}. Jet calibrations are applied as described in Refs. [62,63].

An event is removed if it contains a jet reconstructed with $R = 0.4$ and originating from non-collision backgrounds, which is identified either by a substantial fraction of the jet energy being deposited in known noisy calorimeter cells or by a low fraction of the jet energy being carried by charged particles originating from the primary vertex and lying within a $\Delta R = 0.4$ cone around the jet axis [64]. Rejection of pile-up jets with $|\eta| < 2.4$ and $p_{\text{T}} < 60$ GeV is achieved using a jet-vertex-tagger (JVT) discriminant [65] quantifying the relative probability for a jet to originate from the primary vertex.

The $R = 0.4$ jets containing b-hadrons (b-jets) are identified using the multivariate b-tagging algorithm *MV2c10* [66] based on impact parameters of tracks within the jet cone and positions of secondary decay vertices [67]. The b-tagging efficiency is 77% as measured in simulated $t\bar{t}$ event samples [68].

To discriminate boosted jets originating from W boson decays from those produced through strong interactions, the jet mass obtained by combining measurements from the calorimeter and tracking systems and the substructure variable $D_2^{\beta=1}$ [69,70] are used. The function $D_2^{\beta=1}$ is a ratio of three- to two-point correlation functions based on the p_{T} values and pairwise ΔR separations of jet constituents. The $D_2^{\beta=1}$ variable is specifically sensitive to a two-prong substructure within a jet and tends to zero in a two-body decay limit. A boosted jet is tagged as a W candidate if its mass falls within a certain mass window around m_W and its $D_2^{\beta=1}$ value is sufficiently low. For the W-tagging procedure the mass window and the upper bound placed on $D_2^{\beta=1}$ are tuned, depending on the jet p_{T}, to reach a nominal 50% signal efficiency (W-tag50) with a multi-jet background rejection factor of 40–80 [71,72]. The jet energy and mass are both

calibrated prior to applying the W-tagging discriminant. At the *preselection* level, only the upper bound on $D_2^{\beta=1}$ corresponding to W-tag50 is imposed.

The missing transverse momentum, with magnitude $E_{\mathrm{T}}^{\mathrm{miss}}$, is calculated as the negative vector sum of all reconstructed objects associated with the primary vertex. This includes calibrated electrons, muons, and $R = 0.4$ jets, and a track-based soft term (TST) using ID tracks not associated with the preselected hard objects [73]. The TST is built from tracks with $p_{\mathrm{T}} > 400$ MeV and $|\eta| < 2.5$ which have a sufficient number of hits in the ID, a good fit quality, and an origin consistent with the primary vertex.

Double counting of electrons, muons, and jets reconstructed by more than one lepton and/or jet algorithm as well as misreconstruction of distinct physics objects produced in close proximity are resolved by the overlap removal procedure. The procedure is applied to the *baseline* objects in the following order:

- electron–electron: if two electrons share an ID track then the lower quality electron is removed; if both electrons are of the same quality then the lower-p_{T} electron is removed;
- electron–muon: remove the electron which shares an ID track with the muon;
- electron–jet with $R = 0.4$: remove the jet if $\Delta R(e, \mathrm{jet}) < 0.2$ and, in the $e\nu J$ channel only, the jet is not b-tagged; after repeating this step for all pairs of electrons and surviving jets, electrons within $\Delta R = 0.4$ of a jet are removed;
- muon–jet with $R = 0.4$: if $\Delta R(\mu, \mathrm{jet}) < 0.2$ and the jet has less than three ID tracks originating from the muon production vertex and, in the $e\nu J$ channel only, the jet is not b-tagged, then the jet is removed; after repeating this step for all pairs of muons and surviving jets, muons within $\Delta R = 0.4$ of a jet are removed.

The second overlap removal procedure applied only in the $e\nu J$ channel involves *baseline* electrons and *final* boosted jets. The boosted jet is removed if a *baseline* electron is present within $\Delta R = 1.0$ of the boosted jet direction.

One of the background sources common to both channels is a misidentification of hadronic jets, photon conversions in the material or electrons from hadron decays as prompt electrons, referred to as the fake-electron background (Sect. 5). As this background is estimated in a data-driven way, to avoid double counting, the selected electrons in simulated background events are required to coincide with electrons from the event generators (referred to as 'truth matching' in Table 2).

Table 3 Relative contributions of background processes to the total number of *preselected* background events. The event yields are normalized to the theoretical cross sections. Contributions included into the fake-electron background are denoted by "—". The 'fake electron' row includes all sources of events with misidentified electrons. These events are vetoed in the simulated event samples to prevent double counting

	$eejj$ [%]	$e\nu J$ [%]
$Z/\gamma^*(\to ee)$ + jets	79	< 1
$Z/\gamma^*(\to \tau\tau)$ + jets	< 1	< 1
$W(\to e\nu)$ + jets	–	27
$W(\to \tau\nu)$ + jets	–	3
$t\bar{t}$	16	58
Single-top	1	6
Fake electron	2	2
Diboson	2	4

To correct for differences in various object reconstruction and identification efficiencies between the data and simulated event samples, the simulated events are weighted to correct for differences in the trigger, object reconstruction and identification efficiencies between the data and simulation [57,59,68]. The correction weights are estimated using measurements in control data samples and are typically consistent with unity to within 5%.

5 Background composition

Background processes in the $eejj$ final state are dominated by high-mass Drell–Yan $Z/\gamma^*(\to ee)$ + jets and $t\bar{t} \to bW(e\nu)bW(e\nu)$ production. Contributions from single-top, diboson, $Z/\gamma^*(\to \tau\tau)$ + jets, $W(\to e\nu)$ + jets, and multi-jet production are subdominant. The $W(\to e\nu)$ + jets and multi-jet backgrounds contribute to the $eejj$ sample through misidentification of jets as electrons.

The dominant backgrounds in the $e\nu J$ channel are due to the production of a W boson in association with jets $W(\to e\nu)$ + jets and $t\bar{t} \to bW(e\nu)bW(J)$ followed by single-top, $Z/\gamma^*(\to ee/\tau\tau)$ + jets, $W(\to \tau\nu)$ + jets, diboson, and multi-jet background production. The only sizeable source of events with a misidentified electron is the multi-jet production.

The overall background composition in the $eejj$ and $e\nu J$ *preselected* event samples is shown in Table 3.

Background processes with real electrons are predicted using the simulated event samples. Backgrounds with misidentified electrons are evaluated with a data-driven matrix method as in Ref. [74].

6 Analysis strategy

The analysis is based on measurements of event yields in a number of phase-space regions defined by the discriminating variables described below. Signal regions (SRs) are constructed to maximize sensitivity to the signal process as predicted by the benchmark model for given values of m_{e^*}, in the presence of the SM background. The signal selection efficiency is nearly independent of Λ, and therefore the SRs are optimized for the different values of m_{e^*} instead of using a two-dimensional Λ–m_{e^*} signal optimization. Simulated dominant background processes are constrained in dedicated control regions (CRs). The analysis is blind, and to verify the background predictions after they are constrained by the CRs and before the SRs are unblinded, validation regions (VRs) serve as transitions between CRs and SRs. Signal contamination of all CRs and VRs is negligible. The following section discusses the selection criteria used in the various SRs, CRs, and VRs, which do not overlap.

6.1 Signal regions

The SRs for the $eejj$ channel are constructed using the $m_{\ell\ell}$, S_{T}, $m_{\ell\ell jj}$ discriminating variables, where

- $m_{\ell\ell}$ is the invariant mass of the electron pair,
- S_{T} is the scalar sum of the transverse momenta of the two electrons and the two jets with the highest p_{T}, and
- $m_{\ell\ell jj}$ is the invariant mass of the two electrons and the two jets with the highest p_{T}.

The definition of the SRs is identical to the one used in the search for a singly produced excited muon decaying into a muon and two jets at $\sqrt{s} = 8$ TeV with the ATLAS detector [22]. Further optimization of the $eejj$ channel SRs does not result in a conclusive improvement of sensitivity to the signal process compared to the initial SR definition given in Ref. [22]. The distributions of the discriminating variables for the $eejj$ channel are shown in Fig. 3 after applying the *preselection* requirements (Table 2) and performing a background-only fit in the corresponding CRs.

The selection criteria for the SRs as well as the selection efficiencies for the $eejj$ channel are shown in Table 4.

The SRs in the $e\nu J$ channel are optimized with discriminating variables at each value of m_{e^*} by maximization of the modified significance defined in Ref. [75] as

$$Z = \sqrt{2 \times ((S+B) \times \ln(1+S/B) - S)},$$

where S is the signal yield and B is the background yield in the defined region. This method is checked with minimization of expected upper limit for cross section of the signal, which gives a similar result. The maximization is performed by varying the criteria on the set of variables found to provide a maximum discrimination between the signal and the background, $m_{\mathrm{T}}^{\nu W}$ and $\left|\Delta\phi(e, \vec{E}_{\mathrm{T}}^{\mathrm{miss}})\right|$, simultaneously, where:

- $m_{\mathrm{T}}^{\nu W}$ coincides with the transverse mass of the system of the missing transverse momentum and the W boson in signal events and is given by

$$m_{\mathrm{T}}^{\nu W} = \sqrt{(m_W)^2 + 2 \times \left(\sqrt{(m_W)^2 + (p_{\mathrm{T}}^W)^2} \times E_{\mathrm{T}}^{\mathrm{miss}} - p_x^W \times E_x^{\mathrm{miss}} - p_y^W \times E_y^{\mathrm{miss}}\right)},$$

  where $p_{x(y)}^W$ is the $x(y)$-component of the momentum of the W boson candidate reconstructed as the $R = 1.0$ jet. The $m_{\mathrm{T}}^{\nu W}$ is required to exceed a threshold that grows with m_{e^*}.
- $\left|\Delta\phi(e, \vec{E}_{\mathrm{T}}^{\mathrm{miss}})\right|$ coincides with the absolute value of the azimuthal angle between the neutrino and the electron in signal events. This quantity provides discrimination between signal events and SM processes involving the leptonic decay of a W boson.

Different sets of selection criteria are examined for each m_{e^*} by applying a maximum or minimum requirement on each of the two variables, i.e., min $m_{\mathrm{T}}^{\nu W}$, max $m_{\mathrm{T}}^{\nu W}$, min $\left|\Delta\phi(e, \vec{E}_{\mathrm{T}}^{\mathrm{miss}})\right|$, and the most effective one is used for the corresponding SR. The distributions of the $m_{\mathrm{T}}^{\nu W}$ and $\left|\Delta\phi(e, \vec{E}_{\mathrm{T}}^{\mathrm{miss}})\right|$, as well as in m_J variables are shown in Fig. 4 for the $e\nu J$ channel after applying the *preselection* requirements and the background-only fit in the CRs as discussed in Sects. 6.2 and 8.

In the $e\nu J$ channel, the observables $m_{\mathrm{T}}^{\nu W}$ and $\left|\Delta\phi(e, \vec{E}_{\mathrm{T}}^{\mathrm{miss}})\right|$ are used to create the nine optimized SRs.

Each SR targets a model with a given mass of the excited electron. The SR is defined by applying the *preselection* introduced in Sect. 4 and additionally requiring the criteria defined in Table 5, which include a b-jet veto and selection on $m_{\mathrm{T}}^{\nu W}$ and $\left|\Delta\phi(e, \vec{E}_{\mathrm{T}}^{\mathrm{miss}})\right|$. The large-$R$ jet also passes the 50% signal efficiency requirement on m_J from the W-tagger.

6.2 Control regions

The control regions are used to derive normalization factors and to constrain systematic uncertainties in the respective background yields (Sect. 8). The CRs are defined so as to ensure a high purity in the corresponding background processes and a sufficient number of events, while having no overlap with events in the respective SRs. To ensure that extrapolation uncertainties are small, the selection criteria for the CRs closely follow those used in the corresponding SRs. An individual selection criterion is changed to enrich the background of interest while ensuring no overlap with the

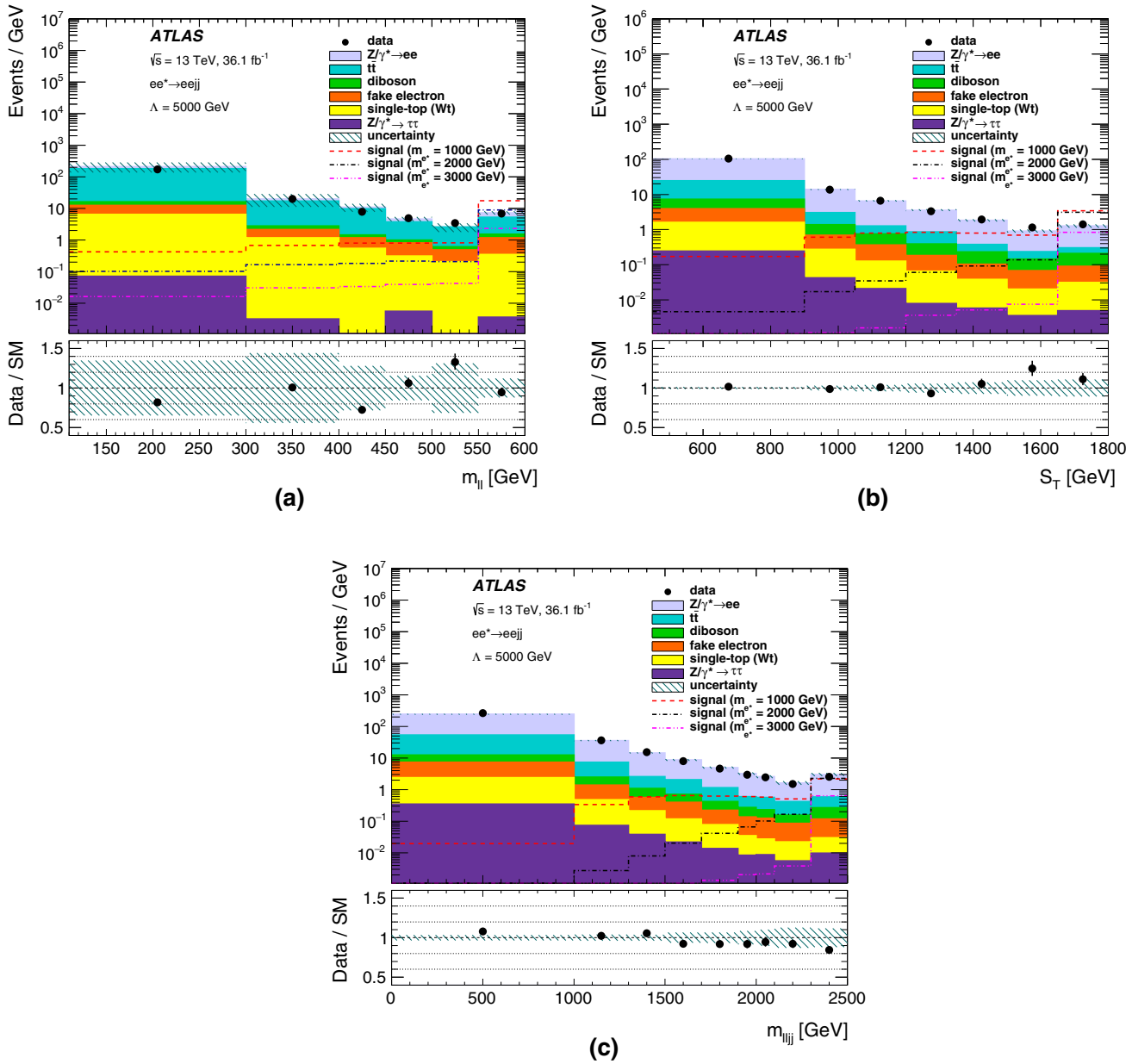

Fig. 3 The distributions of **a** $m_{\ell\ell}$, **b** S_{T}, and **c** $m_{\ell\ell jj}$ used to discriminate the signal from background processes in the $eejj$ channel. The distributions are shown after applying the *preselection* criteria. The background contributions are constrained using the CRs. The signal models assume $\Lambda = 5$ TeV. The last bin includes overflow events (the underflow is not shown). The ratio of the number of data events to the expected number of background events with its statistical uncertainty is shown in the lower panes. The hashed bands represent all considered sources of systematic and statistical uncertainties in the SM background expectation

signal region. Hence, separate control regions are defined for each signal region. The other selection criteria are the same as for the signal regions.

The CRs of the $eejj$ channel (Table 6) are introduced for the two largest sources of background, Z/γ^*+jets and $t\bar{t}$. The Z/γ^* CRs are defined by requiring $|m_{\ell\ell} - m_Z| < 20$ GeV and the same S_{T} and $m_{\ell\ell jj}$ selections as in the corresponding SRs. The $t\bar{t}$ CRs are defined by the full SR selections but at the *preselection* require a single-muon trigger and exactly one electron and exactly one muon in the event, leading to an $e\mu jj$ signature. The kinematic criteria used for the $e\mu jj$ signature (apart from the lepton preselection) are identical to those in the nominal $eejj$ SR selection.

The CRs for the $e\nu J$ channel (Table 7) are defined for the W + jets and $t\bar{t}$ background processes. The W CR is defined by applying the same selection requirements as in

Table 4 Selection requirements for the SRs used to test various mass hypotheses in the $eejj$ channel. They are applied to the *preselected* event samples (see Table 2). Signal efficiencies are presented as the number of signal events in each SR relative to that after the *preselection* and relative to that before any selection. Each signal region is valid for one or more mass hypotheses, as shown in the second column

	m_{e^*} (GeV)	min $m_{\ell\ell}$ (GeV)	min S_{T} (GeV)	min $m_{\ell\ell jj}$ (GeV)	Efficiency relative to *preselection* stage (%)	Total efficiency (%)
SR1	100	500	450	0	36	2
	200				51	10
SR2	300	550	900	1000	41	13
	400				47	18
	500				52	24
	600				57	28
	700				62	33
SR3	800	450	900	1300	68	37
	900				73	41
SR4	1000	450	1050	1300	73	43
SR5	1250	450	1200	1500	77	46
SR6	1500	400	1200	1700	83	52
SR7	1750	300	1350	1900	87	55
SR8	2000	300	1350	2000	91	57
SR9	2250	300	1500	2100	91	58
SR10	2500	110	1650	2300	94	60
	2750				96	61
	3000				97	62
	3250				97	62
	3500				98	62
	3750				98	62
	4000				98	62

the SRs (Table 5), including the b-jet veto, but requiring the jets to fail the boosted jet mass W-tagger with the 80% signal efficiency (W-tag80). Also, the $\left|\Delta\phi(e, \vec{E}_{\mathrm{T}}^{\mathrm{miss}})\right|$ selection is removed for all W CRs in order to reduce the statistical uncertainties. There is no W CR corresponding to SR1 since the W + jets background process is subdominant in such a CR. The $t\bar{t}$ CR events are required to have at least two b-jets, fulfil the respective SR selections from Table 5, and have a leading large-R jet satisfying the m_J W-tag50 criterion. No additional requirements on the kinematic properties of the b-jets are applied in the $t\bar{t}$ CR. The $t\bar{t}$ background prediction is corrected for the difference in b-jet identification efficiencies between data and simulated events, and the corresponding systematic uncertainties are accounted for. Theoretical uncertainties in the $t\bar{t}$ kinematic distributions are accounted for as described in Sect. 7.

6.3 Validation regions

The background estimation in the CRs is validated in additional phase space regions, the VRs. The VRs are not included in any fits aimed at a signal search.

In the $eejj$ channel, a $m_{\ell\ell}$ VR is defined as the intermediate range between SR and Z/γ^* CR. A further requirement on the $E_{\mathrm{T}}^{\mathrm{miss}}$ is introduced to split the $m_{\ell\ell}$ VR into regions dominated by Z/γ^* and $t\bar{t}$ processes. A same-sign (SS) VR is defined in order to validate the fake-electron background estimate by selecting events with $m_{\ell\ell} > 160$ GeV in which both electrons are required to have the same electric charge Q_e (Table 6).

The m_J and b-jet VRs are introduced for the evJ channel. The m_J VRs are defined by applying the *preselection* requirements while inverting the requirement on the boosted jet mass W-tagger interval relative to the W CRs and SRs (Table 7). The b-jet VRs require the number of b-jets to be equal to one to validate the application of $t\bar{t}$ normalization derived in $t\bar{t}$ CR with the two b-jets requirement to the SR with zero b-jets. The requirements on $m_{\mathrm{T}}^{\nu W}$ and $\left|\Delta\phi(e, \vec{E}_{\mathrm{T}}^{\mathrm{miss}})\right|$ in the VRs are the same as in the corresponding SRs.

7 Systematic uncertainties

The systematic uncertainties of the search are divided into two categories: the experimental uncertatinties and theoretical uncertainties in signal and background prediction. Details of the evaluation of experimental uncertainties are provided in the references in Sect. 4.

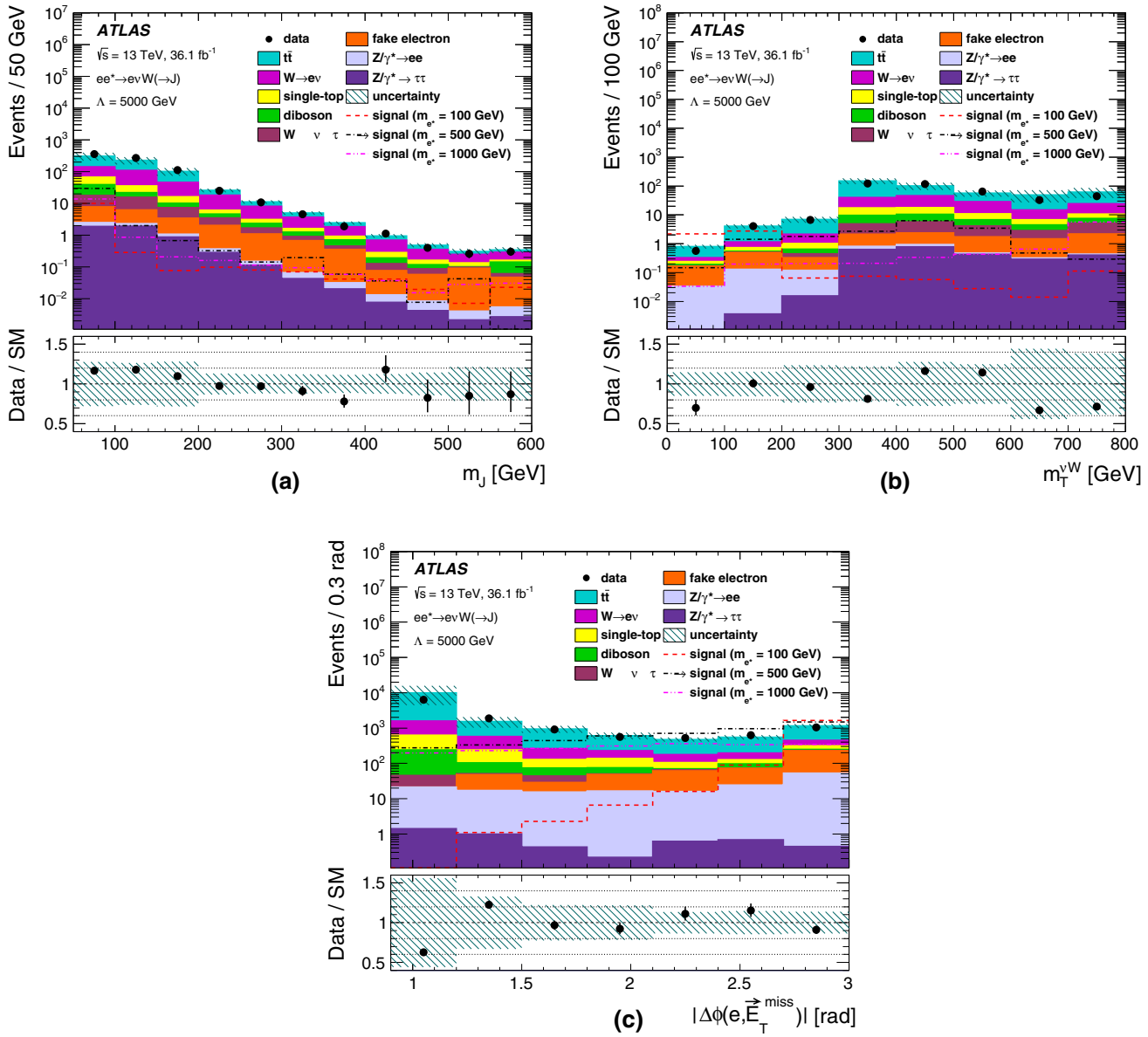

Fig. 4 The distributions of **a** m_J, **b** $m_{\mathrm{T}}^{\nu W}$, and **c** $\left|\Delta\phi(e, \vec{E}_{\mathrm{T}}^{\mathrm{miss}})\right|$ used to discriminate the signal and background processes in the $e\nu J$ channel. The distributions are shown after applying the *preselection* criteria. The background contributions are constrained using the CRs. The signal models assume $\Lambda = 5$ TeV. The last bin includes overflow events (the underflow is not shown). The ratio of the number of data events to the expected number of background events is shown with its statistical uncertainty in the lower panes. The hashed bands represent all considered sources of systematic and statistical uncertainties for the expected backgrounds

The uncertainty in the combined 2015+2016 integrated luminosity is 2.1%. It is derived from the calibration of the luminosity scale using x-y beam-separation scans, following a methodology similar to that detailed in Ref. [76], and using the LUCID-2 detector for the baseline luminosity measurements [77].

The uncertainties in the electron energy scale and resolution result in less than a 1% effect for simulated background or signal event yields in the SRs. In addition, uncertainties are taken into account for the electron trigger ($< 2\%$), identification ($< 3\%$), and reconstruction ($< 1\%$) efficiencies, and for the isolation requirements ($< 6\%$).

The effect of the uncertainty in the muon momentum on $t\bar{t}$ background event yields in the $t\bar{t}$ CRs of the $eejj$ channel does not exceed 1%. Differences between data and simulated event samples in the muon identification and trigger efficiencies are also taken into account and are less than 1%.

Table 5 Selection requirements for the SRs used to test various mass hypotheses in the $e\nu J$ channel. They are applied to discriminating variables after the *preselection* (Table 2) criteria. Signal efficiencies are presented as the number of signal events in each SR relative to that after the *preselection* and relative to that before any selection. Each signal region is valid for one or more mass hypotheses, as shown in the second column. "N/A" means the requirement is not applied for that SR

	m_{e^*} (GeV)	Min $m_{\mathrm{T}}^{\nu W}$ (GeV)	Max $m_{\mathrm{T}}^{\nu W}$ (GeV)	Min $\left\lvert\Delta\phi(e, \vec{E}_{\mathrm{T}}^{\mathrm{miss}})\right\rvert$ (radian)	Efficiency relative to *preselection* stage (%)	Total efficiency (%)
SR1	100	0	200	2.7	61	3
SR2	200	100	N/A	2.4	59	4
SR3	300	100	N/A	2.1	56	5
SR4	400	200	N/A	1.8	40	5
SR5	500	300	N/A	1.5	38	5
SR6	600	400	N/A	1.2	38	6
SR7	700	500	N/A	1.2	34	6
SR8	800	600	N/A	0.9	36	7
	900				38	8
SR9	1000	700	N/A	0.9	37	8
	1250				42	9
	1500				43	10
	1750				44	10
	2000				45	10
	2250				45	10
	2500				43	10
	2750				44	10
	3000				44	10
	3250				42	10
	3500				43	10
	3750				42	10
	4000				42	9

The impact of the $R = 0.4$ jet energy scale (JES) and resolution (JER) uncertainties on the background event yields is 1–5% (JES) and 1–6% (JER) in the SRs of the $eejj$ channel. The signal selection efficiency change in the SRs of the $eejj$ channel due to the JES uncertainties never exceeds 2%, while the effect of the JER uncertainty is negligible. Uncertainties associated with $R = 1.0$ jets in the $e\nu J$ channel arise from uncertainties in the calibration of the JES and the jet mass scale. The impact on the background event yields in the SRs ranges between 20% and 40%, and the effect on signal yields is below 10%. Uncertainties related to the b-tagging efficiency corrections are also taken into account in the $e\nu J$ channel, and the effect on $t\bar{t}$ yields is always below 5%.

The procedure to estimate fake-electron background includes a systematic uncertainty, which is 10–40% of the fake-electron background estimate in the SRs, depending on the p_{T} of the electron candidates.

Theoretical uncertainties affect the simulated event samples of backgrounds and signal. For the background samples, they lie in the PDF set, the value of α_S, and missing higher order corrections in perturbative calculations. The latter effect is estimated by varying the renormalization and factorization scales by factors of one-half and two, excluding those variations where both differ by factor of four. The PDF uncertainty is estimated using the envelope of the NNPDF3.0 PDF set [78] and the two alternative PDF sets, the MMHT2014 [79] and CT14nnlo [80]. The uncertainty due to α_S is estimated by varying its nominal value of 0.118 by ± 0.001. For the $t\bar{t}$ background, the theoretical uncertainty also includes effects of the matching between ME and PS via the variation of the POWHEG-BOX h_{damp} parameter. The effects of the ME and hadronization model choice are assessed for $t\bar{t}$ and single-top MC samples by replacing the POWHEG-BOX ME by aMC@NLO [81] and the PYTHIA 8 hadronization model by the one implemented in HERWIG 7 [82]. The theoretical uncertainties in the signal prediction are estimated using the PDF set variations only. The theoretical uncertainties for background yields range from 7% to 22% in the SRs of the $eejj$ channel and from 3% to 10% in the SRs of the $e\nu J$ channel.

Table 6 Selection requirements applied in addition to the *preselection* (Table 2) in the CRs, VRs, and SRs for the $eejj$ channel. "Pass", 'fail" or "N/A" mean that the requirement is passed, failed or not applied, respectively

Region	Leptons	$m_{\ell\ell}$	S_{T}	$m_{\ell\ell jj}$	Q_e
SR	2 electrons	Pass	Pass	Pass	N/A
Z/γ^* CR	2 electrons	$>$ 70 GeV and $<$ 110 GeV	Pass	Pass	N/A
$t\bar{t}$ CR	1 electron and 1 muon	Pass	Pass	Pass	N/A
$m_{\ell\ell}$ VR	2 electrons	$>$ 110 GeV and $< m_{\ell\ell}^{\text{SR threshold}}$	Pass	Pass	N/A
SS VR	2 electrons	$>$ 160 GeV	N/A	N/A	$Q_{e1} = Q_{e2}$

Table 7 Selection requirements applied in addition to the *preselection* (Table 2) in the CRs, VRs and SRs for the $e\nu J$ channel. "Pass", 'fail" or "N/A" mean that the requirement is passed, failed or not applied, respectively. W-tag80 refers to the working point of the W-tagger with 80% signal efficiency

Region	m_J interval	$N^{b\text{-jets}}$	$m_{\mathrm{T}}^{\nu W}$	$\lvert\Delta\phi(e, \vec{E}_{\mathrm{T}}^{\mathrm{miss}})\rvert$
SR	W-tag50 pass	0	Pass	Pass
W CR	W-tag80 fail	0	Pass	N/A
$t\bar{t}$ CR	W-tag50 pass	≥ 2	Pass	Pass
m_J VR	W-tag50 fail W-tag80 pass	N/A	Pass	Pass
b-jet VR	W-tag50 pass	1	Pass	Pass

Table 8 Background normalization factors with 68% confidence intervals after the background-only fit in the CRs. CRs not defined in the $e\nu J$ channel are denoted as "N/A". The β_W normalization factor in the $e\nu J$ SR1 is fixed to unity

	$eejj$		$e\nu J$	
	β_{Z/γ^*}	$\beta_{t\bar{t}}$	β_W	$\beta_{t\bar{t}}$
CR1	$0.94^{+0.04}_{-0.04}$	$0.95^{+0.08}_{-0.07}$	N/A	$0.8^{+0.2}_{-0.2}$
CR2	$0.82^{+0.04}_{-0.04}$	$1.0^{+0.2}_{-0.2}$	$0.79^{+0.08}_{-0.08}$	$0.8^{+0.2}_{-0.2}$
CR3	$0.79^{+0.04}_{-0.04}$	$0.8^{+0.2}_{-0.2}$	$0.79^{+0.08}_{-0.08}$	$0.8^{+0.2}_{-0.2}$
CR4	$0.81^{+0.05}_{-0.05}$	$0.8^{+0.3}_{-0.3}$	$0.77^{+0.10}_{-0.10}$	$1.0^{+0.4}_{-0.3}$
CR5	$0.80^{+0.06}_{-0.05}$	$1.3^{+0.5}_{-0.4}$	$0.72^{+0.10}_{-0.10}$	$1.2^{+0.5}_{-0.4}$
CR6	$0.76^{+0.06}_{-0.06}$	$1.4^{+0.5}_{-0.5}$	$0.83^{+0.10}_{-0.10}$	$0.7^{+0.4}_{-0.4}$
CR7	$0.78^{+0.07}_{-0.07}$	$1.0^{+0.6}_{-0.5}$	$0.91^{+0.11}_{-0.18}$	$0.13^{+1.17}_{-0.13}$
CR8	$0.74^{+0.07}_{-0.07}$	$1.2^{+0.8}_{-0.7}$	$0.65^{+0.15}_{-0.22}$	$1.7^{+1.6}_{-0.9}$
CR9	$0.64^{+0.08}_{-0.07}$	$1.4^{+1.1}_{-0.9}$	$0.66^{+0.14}_{-0.20}$	$1.6^{+1.6}_{-0.9}$
CR10	$0.62^{+0.10}_{-0.09}$	$1.3^{+0.7}_{-0.5}$	N/A	N/A

8 Statistical analysis and results

The statistical analysis of the search is based on a maximum-likelihood fit. The signal hypothesis test is performed using a likelihood-ratio test statistic in the asymptotic approach [75].

The likelihood function is constructed as the product of Poisson probabilities of the SR and the CRs as in Ref. [83]. The normalizations of the backgrounds which have CRs, i.e., $Z/\gamma^* +$ jets and $t\bar{t}$ for the $eejj$ channel and $W +$ jets and $t\bar{t}$ for the $e\nu J$ channel, are free parameters, denoted by β, in the fit. These corrections are used to scale the background predictions in the SRs. Their values and uncertainties after the background-only fit in the CRs are summarized in Table 8. The deviation of the β values from unity reflects the fact that at high S_{T} the simulated events do not accurately describe the data. This is also observed, for example, in the leptoquark search by ATLAS [84]. After the fit in the corresponding CR, the background yields agree with the data in all VRs within the uncertainties. The final fit combining CRs and SRs results in negligible shifts of the background normalization factors with respect to the CR-only fits. Systematic uncertainties are incorporated into the likelihood function with a set of nuisance parameters with Gaussian constraint terms. Statistical uncertainties from the simulated event samples are included as nuisance parameters with Poisson constraint terms. Correlations of the systematic uncertainty effects across regions are taken into account. The signal normalization (strength) is obtained by maximizing the likelihood function for each

Table 9 Event yields in the signal regions of the $eejj$ channel. Data are shown together with the background contributions after a combined background-only fit in the control and signal regions

Yields	SR1	SR2	SR3	SR4	SR5	SR6	SR7	SR8	SR9	SR10
Observed	448	102	94	62	37	32	32	27	16	15
Background	430 ± 50	110 ± 15	96 ± 10	71 ± 8	43 ± 6	40 ± 5	29 ± 5	275	18 ± 3	21 ± 3
$Z/\gamma^* \to ee$	100 ± 20	48 ± 10	37 ± 6	30 ± 5	16 ± 2	14 ± 2	10 ± 2	9 ± 2	5.4 ± 1.1	8.0 ± 1.3
$t\bar{t}$	230 ± 30	33 ± 7	24 ± 6	14 ± 5	12 ± 4	11 ± 4	6 ± 4	7 ± 4	4 ± 3	5 ± 2
Single-top (Wt)	24 ± 3	7.8 ± 0.8	9.2 ± 1.0	7.3 ± 0.7	4.1 ± 0.4	4.6 ± 0.4	3.0 ± 0.3	2.4 ± 0.3	1.6 ± 0.2	1.50 ± 0.14
Fake electron	50 ± 9	14 ± 2	18 ± 2	15 ± 2	7.2 ± 0.8	7.5 ± 0.9	6.9 ± 0.7	6.7 ± 0.6	4.9 ± 0.5	4.7 ± 0.5
Diboson	21 ± 7	6 ± 2	8 ± 2	6 ± 2	3.8 ± 1.1	3.6 ± 1.0	3.0 ± 0.8	2.6 ± 0.7	1.8 ± 0.5	2.5 ± 0.7
$Z/\gamma^* \to \tau\tau$	0.22 ± 0.09	0.12 ± 0.04	0.12 ± 0.04	0.04 ± 0.01	0.03 ± 0.01	0.03 ± 0.01	0.03 ± 0.01	0.03 ± 0.01	0.01 ± 0.01	0.04 ± 0.02

Table 10 Event yields in the signal regions of the $e\nu J$ channel. Data are shown together with the background contributions after a combined background-only fit in the control and signal regions

Yields	SR1	SR2	SR3	SR4	SR5	SR6	SR7	SR8	SR9
Observed	13	25	39	35	43	34	15	16	8
Background	13 ± 5	17 ± 5	26 ± 8	25 ± 5	34 ± 8	30 ± 6	12 ± 4	8 ± 2	6 ± 2
$W \to e\nu$	2 ± 2	7 ± 3	11 ± 4	13 ± 3	14 ± 5	17 ± 4	7 ± 3	3.2 ± 1.3	2.2 ± 1.1
$Z/\gamma^* \to ee$	1.3 ± 1.2	1.6 ± 1.1	2.1 ± 1.3	1.7 ± 1.0	1.4 ± 0.9	0.6 ± 0.3	0.14 ± 0.10	0.10 ± 0.05	0.04 ± 0.03
$t\bar{t}$	2.9 ± 1.2	5 ± 2	7 ± 3	4 ± 3	11 ± 5	3 ± 2	0.1 ± 0.3	1 ± 2	0.4 ± 0.7
Single-top	0.7 ± 0.3	1.9 ± 0.5	2.6 ± 0.6	3.0 ± 1.4	3.0 ± 1.4	4 ± 2	1.9 ± 0.7	1.9 ± 0.6	1.7 ± 0.7
Fake electron	6 ± 2	1.9 ± 0.3	3.2 ± 1.0	0.6 ± 0.3	0.25 ± 0.07	0.7 ± 0.3	0.06 ± 0.11	–	–
Diboson	0.0 ± 1.1	0.2 ± 1.1	1 ± 2	2.9 ± 0.9	3.4 ± 0.7	3 ± 2	2 ± 3	1.1 ± 1.1	1.1 ± 1.1
$W \to \tau\nu$	–	–	0.0 ± 0.5	0.1 ± 0.2	0.34 ± 0.10	0.2 ± 0.6	0.21 ± 0.09	0.21 ± 0.08	0.20 ± 0.09
$Z/\gamma^* \to \tau\tau$	0.04 ± 0.02	0.04 ± 0.02	0.06 ± 0.03	0.03 ± 0.02	0.08 ± 0.06	0.06 ± 0.05	0.05 ± 0.06	0.1 ± 0.2	–

signal hypothesis. The statistical analysis is performed using the RooStats [85] and HistFitter [86] software.

The observed and expected yields in the SRs for the $eejj$ and $e\nu J$ channels after the combined maximum-likelihood fits to only background processes in the CRs and SRs are shown in Tables 9 and 10, respectively. When calculating the uncertainties on the expected yields in the SRs, all correlations between the nuisance parameters estimates are taken into account. No significant excess above the expected SM background is observed, and limits on the excited lepton model parameters are set at 95% confidence level (CL), using the CL_s method [87]. The upper limits on the signal production cross section times branching ratio $\sigma \times \mathcal{B}$ as a function of m_{e^*} are presented in Fig. 5a, b for the $eejj$ and $e\nu J$ channels, respectively. The fluctuations observed in the limit for the $e\nu J$ channel for m_{e^*} points below 1 TeV are caused by the selection criteria optimized separately at each mass points.

The lower limits on the compositeness scale parameter Λ as a function of m_{e^*} for the $eejj$ and $e\nu J$ channels are presented in Fig. 6a, b. They are calculated from the upper limits on $\sigma \times \mathcal{B}$, taking into account the $\mathcal{B}$ dependency on both the m_{e^*} and Λ parameters. The limits on Λ in the $eejj$ channel are extrapolated to the values of $m_{e^*} > 4$ TeV, since the signal selection efficiency remains constant for the highest m_{e^*} values in SR10, as is shown in Table 4. A unified likelihood function is constructed for the $eejj$ and $e\nu J$ channels at each m_{e^*} value considered in order to extract a combined limit on Λ as a function of m_{e^*}. The correlations of systematic uncertainty effects between the two search channels are included. The combined limit is presented in Fig. 6c along with the individual limits from the $eejj$ and $e\nu J$ channels as well as the limit set by ATLAS in the $ee\gamma$ search channel at $\sqrt{s} = 8$ TeV[21].

Observed and expected model-independent upper limits on the number of signal events in the signal regions of the $eejj$ and $e\nu J$ channels are shown in Table 11 along with the upper limits on the visible signal cross section, which is defined as the production cross-section times the overall signal efficiency.

9 Conclusion

A search for a singly produced excited electron in association with a SM electron is performed using $eejj$ and $e\nu J$ final states with the ATLAS detector at the LHC. The search

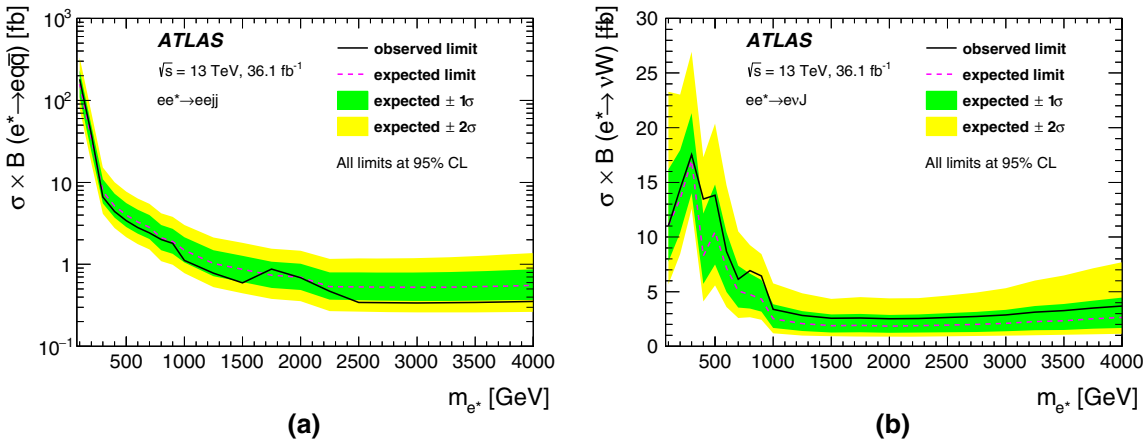

Fig. 5 Upper limits on $\sigma \times \mathcal{B}$ as a function of m_{e^*} in **a** the $eejj$ channel and **b** the $e\nu J$ channel. The $\pm 1(2)\sigma$ uncertainty bands around the expected limit represent all sources of systematic and statistical uncertainties

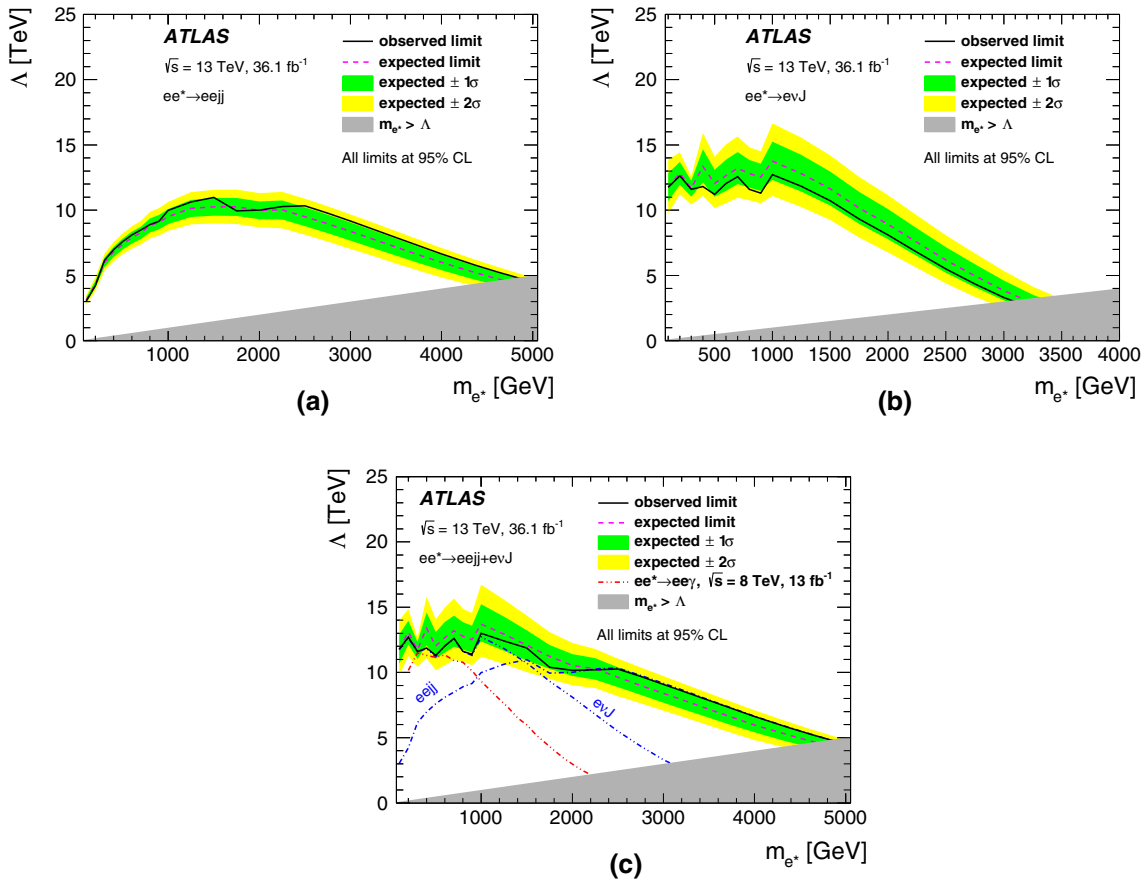

Fig. 6 Lower limits on Λ as a function of m_{e^*} for **a** the $eejj$ channel, **b** the $e\nu J$ channel, and **c** combined limits for both channels. The $\pm 1(2)\sigma$ uncertainty bands around the expected limit represent all sources of systematic and statistical uncertainties. The limits for $m_{e^*} > 4$ TeV are the result of extrapolation. The individual observed lower limits for the $eejj$ (same as **a**) and the $e\nu J$ (same as **b**) channels are shown with the blue dot-and-dash lines in **c** for the reference. The exclusion limit set by ATLAS in the $ee\gamma$ search channel [21] using 13 fb^{-1} of data collected at $\sqrt{s} = 8$ TeV is also shown with the red dotted line in **c**

Table 11 Observed and expected model-independent limits at 95% CL on the number of signal events N_{sig} and the visible cross section σ_{vis} in the signal regions of the $eejj$ and $e\nu J$ channels. The $\pm 1(2)\sigma$ uncertainty intervals around the expected limit represent all sources of systematic and statistical uncertainties. The SR10 is not defined for the $e\nu J$ channel and denoted as "N/A"

	$eejj$				$e\nu J$			
	$N_{\text{sig}}^{\text{obs}}$	$N_{\text{sig}}^{\text{exp}}$	$\sigma_{\text{vis}}^{\text{obs}}$ [fb]	$\sigma_{\text{vis}}^{\text{exp}}$ [fb]	$N_{\text{sig}}^{\text{obs}}$	$N_{\text{sig}}^{\text{exp}}$	$\sigma_{\text{vis}}^{\text{obs}}$ [fb]	$\sigma_{\text{vis}}^{\text{exp}}$ [fb]
SR1	120.3	$107.9^{+38.1(81.6)}_{-29.1(48.8)}$	3.34	$2.99^{+1.06(2.27)}_{-0.81(1.35)}$	11.2	$11.3^{+4.6(10.5)}_{-3.1(5.2)}$	0.31	$0.31^{+0.13(0.29)}_{-0.09(0.14)}$
SR2	30.7	$35.0^{+12.7(27.8)}_{-9.3(15.6)}$	0.85	$0.97^{+0.35(0.77)}_{-0.26(0.43)}$	21.4	$19.9^{+5.9(13.3)}_{-4.2(7.1)}$	0.59	$0.55^{+0.16(0.37)}_{-0.12(0.20)}$
SR3	27.5	$28.7^{+11.1(24.7)}_{-8.0(13.3)}$	0.76	$0.80^{+0.31(0.69)}_{-0.22(0.37)}$	31.6	$30.9^{+7.1(15.9)}_{-5.1(6.6)}$	0.88	$0.86^{+0.20(0.45)}_{-0.14(0.21)}$
SR4	18.1	$23.3^{+9.1(20.4)}_{-6.5(10.7)}$	0.50	$0.64^{+0.25(0.57)}_{-0.18(0.30)}$	23.5	$15.9^{+6.6(14.8)}_{-4.6(7.5)}$	0.65	$0.44^{+0.18(0.41)}_{-0.13(0.21)}$
SR5	13.0	$16.7^{+6.9(15.7)}_{-4.8(7.9)}$	0.36	$0.46^{+0.19(0.44)}_{-0.13(0.22)}$	26.9	$21.1^{+7.9(17.4)}_{-5.7(9.5)}$	0.75	$0.58^{+0.22(0.48)}_{-0.16(0.26)}$
SR6	11.1	$15.8^{+6.6(15.0)}_{-4.6(7.5)}$	0.31	$0.44^{+0.18(0.42)}_{-0.13(0.21)}$	19.9	$17.0^{+6.8(15.4)}_{-4.9(8.0)}$	0.55	$0.47^{+0.19(0.43)}_{-0.13(0.22)}$
SR7	17.0	$14.5^{+6.1(13.9)}_{-4.2(6.9)}$	0.47	$0.40^{+0.17(0.39)}_{-0.12(0.19)}$	13.8	$11.9^{+4.8(10.9)}_{-3.2(5.4)}$	0.38	$0.33^{+0.13(0.30)}_{-0.09(0.15)}$
SR8	14.0	$14.1^{+5.9(13.4)}_{-4.0(6.7)}$	0.39	$0.39^{+0.16(0.37)}_{-0.11(0.18)}$	17.1	$11.9^{+4.6(10.5)}_{-3.1(5.2)}$	0.47	$0.33^{+0.13(0.29)}_{-0.09(0.14)}$
SR9	9.7	$10.9^{+4.8(11.1)}_{-3.2(5.2)}$	0.27	$0.30^{+0.13(0.31)}_{-0.09(0.15)}$	9.4	$7.5^{+3.5(8.3)}_{-2.3(3.7)}$	0.26	$0.21^{+0.10(0.23)}_{-0.06(0.10)}$
SR10	7.3	$11.1^{+4.9(11.4)}_{-3.3(5.4)}$	0.20	$0.31^{+0.14(0.32)}_{-0.09(0.15)}$	N/A	N/A	N/A	N/A

utilizes data from pp collisions at $\sqrt{s} = 13$ TeV with an integrated luminosity of 36.1 fb^{-1}. No significant deviation from the SM background expectation is observed in either channel. Upper limits are calculated for the $pp \to ee^* \to eeq\bar{q}$ and $pp \to ee^* \to e\nu W$ production cross sections as a function of the excited electron mass m_{e^*} at 95% confidence level. Lower limits on the compositeness scale parameter Λ are set at 95% confidence level as a function of m_{e^*}. For excited electrons with $m_{e^*} < 1.5$ TeV, the lower limit on Λ is 11 TeV, and it decreases to 7 TeV at $m_{e^*} = 4$ TeV. In the special case of the excited lepton model where $m_{e^*} = \Lambda$, the values of $m_{e^*} < 4.8$ TeV are excluded. The sensitivity of the search is significantly better than the previous results obtained by ATLAS and CMS from LHC Run 1. Model-independent upper limits on the number of signal events and on the visible signal cross section in the signal regions are presented. The latter vary between 0.20 (0.26) fb and 3.34 (0.88) fb for the $eejj$ ($e\nu J$) channel.

Acknowledgements We thank CERN for the very successful operation of the LHC, as well as the support staff from our institutions without whom ATLAS could not be operated efficiently. We acknowledge the support of ANPCyT, Argentina; YerPhI, Armenia; ARC, Australia; BMWFW and FWF, Austria; ANAS, Azerbaijan; SSTC, Belarus; CNPq and FAPESP, Brazil; NSERC, NRC and CFI, Canada; CERN; CONICYT, Chile; CAS, MOST and NSFC, China; COLCIENCIAS, Colombia; MSMT CR, MPO CR and VSC CR, Czech Republic; DNRF and DNSRC, Denmark; IN2P3-CNRS, CEA-DRF/IRFU, France; SRNSFG, Georgia; BMBF, HGF, and MPG, Germany; GSRT, Greece; RGC, Hong Kong SAR, China; ISF and Benoziyo Center, Israel; INFN, Italy; MEXT and JSPS, Japan; CNRST, Morocco; NWO, Netherlands; RCN, Norway; MNiSW and NCN, Poland; FCT, Portugal; MNE/IFA, Romania; MES of Russia and NRC KI, Russian Federation; JINR; MESTD, Serbia; MSSR, Slovakia; ARRS and MIZŠ, Slovenia; DST/NRF, South Africa; MINECO, Spain; SRC and Wallenberg Foundation, Sweden; SERI, SNSF and Cantons of Bern and Geneva, Switzerland; MOST, Taiwan; TAEK, Turkey; STFC, United Kingdom; DOE and NSF, United States of America. In addition, individual groups and members have received support from BCKDF, CANARIE, CRC and Compute Canada, Canada; COST, ERC, ERDF, Horizon 2020, and Marie Skłodowska-Curie Actions, European Union; Investissements d' Avenir Labex and Idex, ANR, France; DFG and AvH Foundation, Germany; Herakleitos, Thales and Aristeia programmes co-financed by EU-ESF and the Greek NSRF, Greece; BSF-NSF and GIF, Israel; CERCA Programme Generalitat de Catalunya, Spain; The Royal Society and Leverhulme Trust, United Kingdom. The crucial computing support from all WLCG partners is acknowledged gratefully, in particular from CERN, the ATLAS Tier-1 facilities at TRIUMF (Canada), NDGF (Denmark, Norway, Sweden), CC-IN2P3 (France), KIT/GridKA (Germany), INFN-CNAF (Italy), NL-T1 (Netherlands), PIC (Spain), ASGC (Taiwan), RAL (UK) and BNL (USA), the Tier-2 facilities worldwide and large non-WLCG resource providers. Major contributors of computing resources are listed in Ref. [88].

Data Availability Statement This manuscript has no associated data or the data will not be deposited. [Author's comment: All ATLAS scientific output is published in journals, and preliminary results are made available in Conference Notes. All are openly available, without restriction on use by external parties beyond copyright law and the standard conditions agreed by CERN. Data associated with journal publications are also made available: tables and data from plots (e.g. cross section values, likelihood profiles, selection efficiencies, cross section limits, ...) are stored in appropriate repositories such as HEPDATA (http://hepdata.cedar.ac.uk/). ATLAS also strives to make additional material related to the paper available that allows a reinterpretation of the data in the context of new theoretical models. For example, an extended encapsulation of the analysis is often provided for measurements in the framework of RIVET (http://rivet.hepforge.org/)." This information is taken from the ATLAS Data Access Policy, which is a public document that can be downloaded from http://opendata.cern.ch/record/413 [opendata.cern.ch].]

Funded by SCOAP[3].

References

1. J.C. Pati, A. Salam, Lepton number as the fourth "color". Phys. Rev. D **10**, 275 (1974) [Erratum: Phys. Rev. D **11**, 703 (1975)]
2. B. Kayser, R.E. Shrock, Distinguishing between Dirac and Majorana neutrinos in neutral-current reactions. Phys. Lett. B **112**, 137 (1982)
3. E. Eichten, K.D. Lane, M.E. Peskin, New tests for quark and lepton substructure. Phys. Rev. Lett. **50**, 811 (1983)
4. N. Cabibbo, L. Maiani, Y. Srivastava, Anomalous Z decays: excited leptons? Phys. Lett. B **139**, 459 (1984)
5. K. Hagiwara, D. Zeppenfeld, S. Komamiya, Excited lepton production at LEP and HERA. Z. Phys. C **29**, 115 (1985)
6. U. Baur, M. Spira, P.M. Zerwas, Excited-quark and -lepton production at hadron colliders. Phys. Rev. D **42**, 815 (1990)
7. T.B. Anders, R. von Mellenthin, B. Pfeil, H. Selecker, Unitarity bounds for 4-fermion contact interactions. Found. Phys. **23**, 399 (1993)
8. ATLAS Collaboration, Search for new phenomena in events with three or more charged leptons in pp collisions at $\sqrt{s} = 8$ TeV with the ATLAS detector. JHEP **08**, 138 (2015). arXiv: 1411.2921 [hep-ex]
9. ATLAS Collaboration, The ATLAS Experiment at the CERN Large Hadron Collider. JINST **3**, S08003 (2008)
10. ALEPH Collaboration, Search for excited leptons at 130-140 GeV. Phys. Lett. B **385**, 445 (1996)
11. O.P.A.L. Collaboration, Search for unstable heavy and excited leptons at LEP2. Eur. Phys. J. C **14**, 73 (2000). arXiv:hep-ex/0001056
12. L3 Collaboration, Search for excited leptons at LEP. Phys. Lett. B **568**, 23 (2003). arXiv:hep-ex/0306016
13. DELPHI Collaboration, Search for excited leptons in e^+e^- collisions at $\sqrt{s} = 189 - 209$ GeV. Eur. Phys. J. C **46**, 277 (2006). arXiv: hep-ex/0603045
14. Z.E.U.S. Collaboration, Searches for excited fermions in ep collisions at HERA. Phys. Lett. B **549**, 32 (2002). arXiv:hep-ex/0109018
15. H1 Collaboration, Search for excited electrons in ep collisions at HERA. Phys. Lett. B **666**, 131 (2008). arXiv:0805.4530 [hep-ex]
16. CDF Collaboration, Search for Excited and Exotic Electrons in the $e\gamma$ Decay Channel in $p\bar{p}$ collisions at $\sqrt{s} = 1.96$ TeV. Phys. Rev. Lett. **94**, 101802 (2005). arXiv: hep-ex/0410013
17. CDF Collaboration, Search for Excited and Exotic Muons in the $\mu\gamma$ Decay Channel in $p\bar{p}$ collisions at $\sqrt{s} = 1.96$ TeV. Phys. Rev. Lett. **97**, 191802 (2006). arXiv:hep-ex/0606043
18. D0 Collaboration, Search for excited muons in $p\bar{p}$ collisions at $\sqrt{s} = 1.96$ TeV. Phys. Rev. D **73**, 111102 (2006). arXiv:hep-ex/0604040
19. D0 Collaboration, Search for excited electrons in $p\bar{p}$ collisions at $\sqrt{s} = 1.96$ TeV. Phys. Rev. D **77**, 091102 (2008). arXiv:0801.0877 [hep-ex]
20. ATLAS Collaboration, Search for excited leptons in proton–proton collisions at $\sqrt{s} = 7$ TeV with the ATLAS detector. Phys. Rev. D **85**, 072003 (2012). arXiv:1201.3293 [hep-ex]
21. ATLAS Collaboration, Search for excited electrons and muons in $\sqrt{s} = 8$ TeV proton–proton collisions with the ATLAS detector. New J. Phys. **15**, 093011 (2013). arXiv:1308.1364 [hep-ex]
22. ATLAS Collaboration, A search for an excited muon decaying to a muon and two jets in pp collisions at $\sqrt{s} = 8$ TeV with the ATLAS detector. New J. Phys. **18**, 073021 (2016). arXiv:1601.05627 [hep-ex]
23. CMS Collaboration, A search for excited leptons in pp collisions at $\sqrt{s} = 7$ TeV. Phys. Lett. B **704**, 143 (2011). arXiv:1107.1773 [hep-ex]
24. CMS Collaboration, Search for excited leptons in pp collisions at $\sqrt{s} = 7$ TeV. Phys. Lett. B **720**, 309 (2013). arXiv:1210.2422 [hep-ex]
25. CMS Collaboration, Search for excited leptons in proton-proton collisions at $\sqrt{s} = 8$ TeV. JHEP **03**, 125 (2016). arXiv:1511.01407 [hep-ex]
26. CMS Collaboration, Search for excited leptons in $\ell\ell\gamma$ final states in proton-proton collisions at $\sqrt{s} = 13$ TeV. JHEP **04**, 015 (2019). arXiv:1811.03052 [hep-ex]
27. ATLAS Collaboration, ATLAS Insertable B-Layer Technical Design Report, tech. rep., 2010. https://cds.cern.ch/record/1291633 [Addendum: ATLAS Insertable B-Layer Technical Design Report Addendum. (2012), http://cds.cern.ch/record/1451888]
28. B. Abbott et al., Production and integration of the ATLAS Insertable B-Layer. JINST **13**, T05008 (2018). arXiv:1803.00844 [physics.ins-det]
29. ATLAS Collaboration, Performance of the ATLAS trigger system in 2015. Eur. Phys. J. C **77**, 317 (2017). arXiv:1611.09661 [hep-ex]
30. T. Sjöstrand et al., An introduction to PYTHIA 8.2. Comput. Phys. Commun. **191**, 159 (2015). arXiv:1410.3012 [hep-ph]
31. NNPDF Collaboration, R. D. Ball et al., Parton distributions with LHC data. Nucl. Phys. B **867**, 244 (2013). arXiv:1207.1303 [hep-ph]
32. ATLAS Collaboration, ATLAS Pythia 8 tunes to 7 TeV data. Technical report ATL-PHYS-PUB-2014-021, CERN, 2014. https://cds.cern.ch/record/1966419. Accessed 21 Sept 2019
33. A. Belyaev, N.D. Christensen, A. Pukhov, CalcHEP 3.4 for collider physics within and beyond the Standard Model. Comput. Phys. Commun. **184**, 1729 (2013). arXiv:1207.6082 [hep-ph]
34. T. Gleisberg et al., Event generation with SHERPA 1.1. JHEP **02**, 007 (2009). arXiv:0811.4622 [hep-ph]
35. F. Cascioli, P. Maierhofer, S. Pozzorini, Scattering amplitudes with open loops. Phys. Rev. Lett. **108**, 111601 (2012). arXiv:1111.5206 [hep-ph]
36. T. Gleisberg, S. Hoeche, Comix, a new matrix element generator. JHEP **12**, 039 (2008). arXiv:0808.3674 [hep-ph]
37. S. Hoeche, F. Krauss, M. Schonherr, F. Siegert, QCD matrix elements + parton showers. The NLO case. JHEP **04**, 027 (2013). arXiv:1207.5030 [hep-ph]
38. NNPDF Collaboration, R.D. Ball et al., Parton distributions for the LHC Run II. JHEP **04**, 040 (2015). arXiv:1410.8849 [hep-ph]
39. Y. Li, F. Petriello, Combining QCD and electroweak corrections to dilepton production in the framework of the FEWZ simulation code. Phys. Rev. D **86**, 094034 (2012). arXiv:1208.5967 [hep-ph]
40. P. Nason, A new method for combining NLO QCD with shower Monte Carlo algorithms. JHEP **11**, 040 (2004). arXiv:hep-ph/0409146
41. S. Frixione, P. Nason, C. Oleari, Matching NLO QCD computations with parton shower simulations: the POWHEG method. JHEP **11**, 070 (2007). arXiv:0709.2092 [hep-ph]
42. S. Frixione, P. Nason, G. Ridolfi, A positive-weight next-to-leading-order Monte Carlo for heavy flavour hadroproduction. JHEP **09**, 126 (2007). arXiv:0707.3088 [hep-ph]
43. S. Alioli, P. Nason, C. Oleari, E. Re, A general framework for implementing NLO calculations in shower Monte Carlo programs: the POWHEG BOX. JHEP **06**, 043 (2010). arXiv:1002.2581 [hep-ph]
44. H.-L. Lai et al., New parton distributions for collider physics. Phys. Rev. D **82**, 074024 (2010). arXiv:1007.2241 [hep-ph]
45. S. Alioli, P. Nason, C. Oleari, E. Re, NLO single-top production matched with shower in POWHEG: s- and t-channel contri-

butions, JHEP **09**, 111 (2009) [Erratum: JHEP **02**, 011 (2010)]. arXiv:0907.4076 [hep-ph]
46. E. Re, Single-top Wt-channel production matched with parton showers using the POWHEG method. Eur. Phys. J. C **71**, 1547 (2011). arXiv:1009.2450 [hep-ph]
47. T. Sjostrand, S. Mrenna, P.Z. Skands, PYTHIA 6.4 physics and manual. JHEP **05**, 026 (2006). arXiv:hep-ph/0603175
48. P.Z. Skands, Tuning Monte Carlo generators: the Perugia tunes. Phys. Rev. D **82**, 074018 (2010). arXiv:1005.3457 [hep-ph]
49. M. Czakon, A. Mitov, Top++: a program for the calculation of the top-pair cross-section at hadron colliders. Comput. Phys. Commun. **185**, 2930 (2014). arXiv:1112.5675 [hep-ph]
50. N. Kidonakis, Next-to-next-to-leading-order collinear and soft gluon corrections for t-channel single top quark production. Phys. Rev. D **83**, 091503 (2011). arXiv:1103.2792 [hep-ph]
51. D.J. Lange, The EvtGen particle decay simulation package. Nucl. Instrum. Methods A **462**, 152 (2001)
52. T. Sjostrand, S. Mrenna, P.Z. Skands, A brief introduction to PYTHIA 8.1. Comput. Phys. Commun. **178**, 852 (2008). arXiv:0710.3820 [hep-ph]
53. ATLAS Collaboration, Summary of ATLAS Pythia 8 tunes, tech. rep. ATL-PHYS-PUB-2012-003, CERN, 2012. https://cds.cern.ch/record/1474107. Accessed 21 Sept 2019
54. A.D. Martin, W.J. Stirling, R.S. Thorne, G. Watt, Parton distributions for the LHC. Eur. Phys. J. C **63**, 189 (2009). arXiv:0901.0002 [hep-ph]
55. ATLAS Collaboration, The ATLAS simulation infrastructure. Eur. Phys. J. C **70**, 823 (2010). arXiv:1005.4568 [physics.ins-det]
56. S. Agostinelli et al., GEANT4—a simulation toolkit. Nucl. Instrum. Methods A **506**, 250 (2003)
57. ATLAS Collaboration, Electron reconstruction and identification in the ATLAS experiment using the 2015 and 2016 LHC proton-proton collision data at $\sqrt{s} = 13$ TeV. (2019). arXiv:1902.04655 [physics.ins-det]
58. ATLAS Collaboration, Electron and photon energy calibration with the ATLAS detector using 2015-2016 LHC proton-proton collision data. JINST **14**, P03017 (2019). arXiv:1812.03848 [hep-ex]
59. ATLAS Collaboration, Muon reconstruction performance of the ATLAS detector in proton-proton collision data at $\sqrt{s} = 13$ TeV. Eur. Phys. J. C **76**, 292 (2016). arXiv:1603.05598 [hep-ex]
60. M. Cacciari, G.P. Salam, G. Soyez, The anti-k_t jet clustering algorithm. JHEP **04**, 063 (2008). arXiv:0802.1189 [hep-ph]
61. D. Krohn, J. Thaler, L.-T. Wang, Jet trimming. JHEP **02**, 084 (2010). arXiv:0912.1342 [hep-ph]
62. ATLAS Collaboration, Jet energy scale measurements and their systematic uncertainties in proton–proton collisions at $\sqrt{s} = 13$ TeV with the ATLAS detector. Phys. Rev. D **96**, 072002 (2017). arXiv:1703.09665 [hep-ex]
63. ATLAS Collaboration, In situ calibration of large-radius jet energy and mass in 13 TeV proton-proton collisions with the ATLAS detector. Eur. Phys. J. C **79**, 135 (2019). arXiv:1807.09477 [hep-ex]
64. ATLAS Collaboration, Selection of jets produced in 13TeV proton-proton collisions with the ATLAS detector, tech. rep. ATLAS-CONF-2015-029, 2015. https://cds.cern.ch/record/2037702. Accessed 21 Sept 2019
65. ATLAS Collaboration, Performance of pile-up mitigation techniques for jets in pp collisions at $\sqrt{s} = 8$ TeV using the ATLAS detector. Eur. Phys. J. C **76**, 581 (2016). arXiv:1510.03823 [hep-ex]
66. ATLAS Collaboration, Optimisation of the ATLAS b-tagging performance for the 2016 LHC Run, tech. rep. ATL-PHYS-PUB-2016-012, CERN, 2016. https://cds.cern.ch/record/2160731. Accessed 21 Sept 2019
67. ATLAS Collaboration, Performance of b-jet identification in the ATLAS experiment. JINST **11**, P04008 (2016). arXiv:1512.01094 [hep-ex]
68. ATLAS Collaboration, Measurements of b-jet tagging efficiency with the ATLAS detector using $t\bar{t}$ events at $\sqrt{s} = 13$ TeV. JHEP **08**, 089 (2018). arXiv:1805.01845 [hep-ex]
69. A.J. Larkoski, G.P. Salam, J. Thaler, Energy correlation functions for jet substructure. JHEP **06**, 108 (2013). arXiv:1305.0007 [hep-ph]
70. A.J. Larkoski, I. Moult, D. Neill, Power counting to better jet observables. JHEP **12**, 009 (2014). arXiv:1409.6298 [hep-ph]
71. ATLAS Collaboration, Performance of top-quark and W-boson tagging with ATLAS in Run 2 of the LHC. Eur. Phys. J. C **79**, 375 (2019). arXiv:1808.07858 [hep-ex]
72. ATLAS Collaboration, Identification of boosted, hadronically-decaying W and Z bosons in $\sqrt{s} = 13$ TeV Monte Carlo Simulations for ATLAS, tech. rep. ATL-PHYS-PUB-2015-033, CERN, 2015. https://cds.cern.ch/record/2041461. Accessed 21 Sept 2019
73. ATLAS Collaboration, Performance of missing transverse momentum reconstruction with the ATLAS detector using proton-proton collisions at $\sqrt{s} = 13$ TeV. Eur. Phys. J. C **78**, 903 (2018). arXiv:1802.08168 [hep-ex]
74. ATLAS Collaboration, Search for scalar leptoquarks in pp collisions at $\sqrt{s} = 13$ TeV with the ATLAS experiment. New J. Phys. **18**, 093016 (2016). arXiv:1605.06035 [hep-ex]
75. G. Cowan, K. Cranmer, E. Gross, O. Vitells, Asymptotic formulae for likelihood-based tests of new physics. Eur. Phys. J. C **71**, 1554 (2011). arXiv:1007.1727 [physics.data-an] [Erratum: Eur. Phys. J. C 73, 2501 (2013)]
76. ATLAS Collaboration, Luminosity determination in pp collisions at $\sqrt{s} = 8$ TeV using the ATLAS detector at the LHC. Eur. Phys. J. C **76**, 653 (2016). arXiv:1608.03953 [hep-ex]
77. G. Avoni et al., The new LUCID-2 detector for luminosity measurement and monitoring in ATLAS. JINST **13**, P07017 (2018)
78. M. Botje et al., The PDF4LHC working group interim recommendations. (2011). arXiv:1101.0538 [hep-ph]
79. L.A. Harland-Lang, A.D. Martin, P. Motylinski, R.S. Thorne, Parton distributions in the LHC era: MMHT 2014 PDFs. Eur. Phys. J. C **75**, 204 (2015). arXiv:1412.3989 [hep-ph]
80. S. Dulat et al., New parton distribution functions from a global analysis of quantum chromodynamics. Phys. Rev. D **93**, 033006 (2016). arXiv:1506.07443 [hep-ph]
81. S. Frixione, F. Stoeckli, P. Torrielli, B.R. Webber, C.D. White, The MCaNLO 4.0 Event Generator. (2010). arXiv:1010.0819 [hep-ph]
82. M. Bahr et al., Herwig++ physics and manual. Eur. Phys. J. **C58**, 639 (2008). arXiv:0803.0883 [hep-ph]
83. K. Cranmer, G. Lewis, L. Moneta, A. Shibata, W. Verkerke, HistFactory: a tool for creating statistical models for use with RooFit and RooStats. Technical report CERN-OPEN-2012-016, 2012. https://cds.cern.ch/record/1456844. Accessed 21 Sept 2019
84. ATLAS Collaboration, Searches for scalar leptoquarks and differential cross-section measurements in dilepton-dijet events in proton-proton collisions at a centre-of-mass energy of $\sqrt{s} = 13$ TeV with the ATLAS experiment. (2019). arXiv: 1902.00377 [hep-ex]
85. L. Moneta et al., 'The RooStats Project', *Proceedings, 13th International Workshop on Advanced computing and Analysis Techniques in Physics Research (ACAT2010): Jaipur, India, February 22–27, 2010*, vol. ACAT2010, 2010 057. arXiv:1009.1003 [physics.data-an]
86. M. Baak et al., HistFitter software framework for statistical data analysis. Eur. Phys. J. C **75**, 153 (2015). arXiv:1410.1280 [hep-ex]
87. A.L. Read, Presentation of search results: the CL_s technique. J. Phys. G **28**, 2693 (2002)
88. ATLAS Collaboration, ATLAS Computing Acknowledgements, ATL-GEN-PUB-2016-002. https://cds.cern.ch/record/2202407. Accessed 21 Sept 2019

ATLAS Collaboration

M. Aaboud[35d], G. Aad[100], B. Abbott[127], D. C. Abbott[101], O. Abdinov[13,*], B. Abeloos[131], D. K. Abhayasinghe[92], S. H. Abidi[166], O. S. AbouZeid[40], N. L. Abraham[155], H. Abramowicz[160], H. Abreu[159], Y. Abulaiti[6], B. S. Acharya[65a,65b,o], S. Adachi[162], L. Adam[98], C. Adam Bourdarios[131], L. Adamczyk[82a], L. Adamek[166], J. Adelman[120], M. Adersberger[113], A. Adiguzel[12c,ai], T. Adye[143], A. A. Affolder[145], Y. Afik[159], C. Agapopoulou[131], C. Agheorghiesei[27c], J. A. Aguilar-Saavedra[139f,139a,ah], F. Ahmadov[78], G. Aielli[72a,72b], S. Akatsuka[84], T. P. A. Åkesson[95], E. Akilli[53], A. V. Akimov[109], G. L. Alberghi[23b,23a], J. Albert[175], M. J. Alconada Verzini[87], S. Alderweireldt[118], M. Aleksa[36], I. N. Aleksandrov[78], C. Alexa[27b], D. Alexandre[19], T. Alexopoulos[10], M. Alhroob[127], B. Ali[141], G. Alimonti[67a], J. Alison[37], S. P. Alkire[147], C. Allaire[131], B. M. M. Allbrooke[155], B. W. Allen[130], P. P. Allport[21], A. Aloisio[68a,68b], A. Alonso[40], F. Alonso[87], C. Alpigiani[147], A. A. Alshehri[56], M. I. Alstaty[100], B. Alvarez Gonzalez[36], D. Álvarez Piqueras[173], M. G. Alviggi[68a,68b], Y. Amaral Coutinho[79b], A. Ambler[102], L. Ambroz[134], C. Amelung[26], D. Amidei[104], S. P. Amor Dos Santos[139a,139c], S. Amoroso[45], C. S. Amrouche[53], F. An[77], C. Anastopoulos[148], N. Andari[144], T. Andeen[11], C. F. Anders[60b], J. K. Anders[20], A. Andreazza[67a,67b], V. Andrei[60a], C. R. Anelli[175], S. Angelidakis[38], I. Angelozzi[119], A. Angerami[39], A. V. Anisenkov[121b,121a], A. Annovi[70a], C. Antel[60a], M. T. Anthony[148], M. Antonelli[50], D. J. A. Antrim[170], F. Anulli[71a], M. Aoki[80], J. A. Aparisi Pozo[173], L. Aperio Bella[36], G. Arabidze[105], J. P. Araque[139a], V. Araujo Ferraz[79b], R. Araujo Pereira[79b], A. T. H. Arce[48], F. A. Arduh[87], J-F. Arguin[108], S. Argyropoulos[76], J.-H. Arling[45], A. J. Armbruster[36], L. J. Armitage[91], A. Armstrong[170], O. Arnaez[166], H. Arnold[119], A. Artamonov[110,*], G. Artoni[134], S. Artz[98], S. Asai[162], N. Asbah[58], E. M. Asimakopoulou[171], L. Asquith[155], K. Assamagan[29], R. Astalos[28a], R. J. Atkin[33a], M. Atkinson[172], N. B. Atlay[150], K. Augsten[141], G. Avolio[36], R. Avramidou[59a], M. K. Ayoub[15a], A. M. Azoulay[167b], G. Azuelos[108,aw], A. E. Baas[60a], M. J. Baca[21], H. Bachacou[144], K. Bachas[66a,66b], M. Backes[134], F. Backman[44a,44b], P. Bagnaia[71a,71b], M. Bahmani[83], H. Bahrasemani[151], A. J. Bailey[173], V. R. Bailey[172], J. T. Baines[143], M. Bajic[40], C. Bakalis[10], O. K. Baker[182], P. J. Bakker[119], D. Bakshi Gupta[8], S. Balaji[156], E. M. Baldin[121b,121a], P. Balek[179], F. Balli[144], W. K. Balunas[134], J. Balz[98], E. Banas[83], A. Bandyopadhyay[24], Sw. Banerjee[180,j], A. A. E. Bannoura[181], L. Barak[160], W. M. Barbe[38], E. L. Barberio[103], D. Barberis[54b,54a], M. Barbero[100], T. Barillari[114], M-S. Barisits[36], J. Barkeloo[130], T. Barklow[152], R. Barnea[159], S. L. Barnes[59c], B. M. Barnett[143], R. M. Barnett[18], Z. Barnovska-Blenessy[59a], A. Baroncelli[59a], G. Barone[29], A. J. Barr[134], L. Barranco Navarro[173], F. Barreiro[97], J. Barreiro Guimarães da Costa[15a], R. Bartoldus[152], A. E. Barton[88], P. Bartos[28a], A. Basalaev[45], A. Bassalat[131,aq], R. L. Bates[56], S. J. Batista[166], S. Batlamous[35e], J. R. Batley[32], M. Battaglia[145], M. Bauce[71a,71b], F. Bauer[144], K. T. Bauer[170], H. S. Bawa[31,m], J. B. Beacham[125], T. Beau[135], P. H. Beauchemin[169], P. Bechtle[24], H. C. Beck[52], H. P. Beck[20,r], K. Becker[51], M. Becker[98], C. Becot[45], A. Beddall[12d], A. J. Beddall[12a], V. A. Bednyakov[78], M. Bedognetti[119], C. P. Bee[154], T. A. Beermann[75], M. Begalli[79b], M. Begel[29], A. Behera[154], J. K. Behr[45], F. Beisiegel[24], A. S. Bell[93], G. Bella[160], L. Bellagamba[23b], A. Bellerive[34], M. Bellomo[159], P. Bellos[9], K. Beloborodov[121b,121a], K. Belotskiy[111], N. L. Belyaev[111], O. Benary[160,*], D. Benchekroun[35a], N. Benekos[10], Y. Benhammou[160], E. Benhar Noccioli[182], D. P. Benjamin[6], M. Benoit[53], J. R. Bensinger[26], S. Bentvelsen[119], L. Beresford[134], M. Beretta[50], D. Berge[45], E. Bergeaas Kuutmann[171], N. Berger[5], B. Bergmann[141], L. J. Bergsten[26], J. Beringer[18], S. Berlendis[7], N. R. Bernard[101], G. Bernardi[135], C. Bernius[152], F. U. Bernlochner[24], T. Berry[92], P. Berta[98], C. Bertella[15a], G. Bertoli[44a,44b], I. A. Bertram[88], G. J. Besjes[40], O. Bessidskaia Bylund[181], N. Besson[144], A. Bethani[99], S. Bethke[114], A. Betti[24], A. J. Bevan[91], J. Beyer[114], R. Bi[138], R. M. Bianchi[138], O. Biebel[113], D. Biedermann[19], R. Bielski[36], K. Bierwagen[98], N. V. Biesuz[70a,70b], M. Biglietti[73a], T. R. V. Billoud[108], M. Bindi[52], A. Bingul[12d], C. Bini[71a,71b], S. Biondi[23b,23a], M. Birman[179], T. Bisanz[52], J. P. Biswal[160], A. Bitadze[99], C. Bittrich[47], D. M. Bjergaard[48], J. E. Black[152], K. M. Black[25], T. Blazek[28a], I. Bloch[45], C. Blocker[26], A. Blue[56], U. Blumenschein[91], S. Blunier[146a], G. J. Bobbink[119], V. S. Bobrovnikov[121b,121a], S. S. Bocchetta[95], A. Bocci[48], D. Boerner[45], D. Bogavac[113], A. G. Bogdanchikov[121b,121a], C. Bohm[44a], V. Boisvert[92], P. Bokan[52,171], T. Bold[82a], A. S. Boldyrev[112], A. E. Bolz[60b], M. Bomben[135], M. Bona[91], J. S. Bonilla[130], M. Boonekamp[144], H. M. Borecka-Bielska[89], A. Borisov[122], G. Borissov[88], J. Bortfeldt[36], D. Bortoletto[134], V. Bortolotto[72a,72b], D. Boscherini[23b], M. Bosman[14], J. D. Bossio Sola[30], K. Bouaouda[35a], J. Boudreau[138], E. V. Bouhova-Thacker[88], D. Boumediene[38], S. K. Boutle[56], A. Boveia[125], J. Boyd[36], D. Boye[33b], I. R. Boyko[78], A. J. Bozson[92], J. Bracinik[21], N. Brahimi[100], G. Brandt[181], O. Brandt[60a], F. Braren[45], U. Bratzler[163], B. Brau[101], J. E. Brau[130], W. D. Breaden Madden[56], K. Brendlinger[45], L. Brenner[45], R. Brenner[171], S. Bressler[179], B. Brickwedde[98], D. L. Briglin[21], D. Britton[56], D. Britzger[114], I. Brock[24], R. Brock[105], G. Brooijmans[39], T. Brooks[92], W. K. Brooks[146b], E. Brost[120], J. H. Broughton[21], P. A. Bruckman de Renstrom[83], D. Bruncko[28b], A. Bruni[23b], G. Bruni[23b], L. S. Bruni[119], S. Bruno[72a,72b], B. H. Brunt[32], M. Bruschi[23b], N. Bruscino[138], P. Bryant[37], L. Bryngemark[95], T. Buanes[17], Q. Buat[36], P. Buchholz[150], A. G. Buckley[56], I. A. Budagov[78], M. K. Bugge[133], F. Bührer[51], O. Bulekov[111], T. J. Burch[120], S. Burdin[89], C. D. Burgard[119],

A. M. Burger[5], B. Burghgrave[8], K. Burka[83], I. Burmeister[46], J. T. P. Burr[134], V. Büscher[98], E. Buschmann[52], P. J. Bussey[56], J. M. Butler[25], C. M. Buttar[56], J. M. Butterworth[93], P. Butti[36], W. Buttinger[36], A. Buzatu[157], A. R. Buzykaev[121b,121a], G. Cabras[23b,23a], S. Cabrera Urbán[173], D. Caforio[141], H. Cai[172], V. M. M. Cairo[2], O. Cakir[4a], N. Calace[36], P. Calafiura[18], A. Calandri[100], G. Calderini[135], P. Calfayan[64], G. Callea[56], L. P. Caloba[79b], S. Calvente Lopez[97], D. Calvet[38], S. Calvet[38], T. P. Calvet[154], M. Calvetti[70a,70b], R. Camacho Toro[135], S. Camarda[36], D. Camarero Munoz[97], P. Camarri[72a,72b], D. Cameron[133], R. Caminal Armadans[101], C. Camincher[36], S. Campana[36], M. Campanelli[93], A. Camplani[40], A. Campoverde[150], V. Canale[68a,68b], M. Cano Bret[59c], J. Cantero[128], T. Cao[160], Y. Cao[172], M. D. M. Capeans Garrido[36], M. Capua[41b,41a], R. M. Carbone[39], R. Cardarelli[72a], F. C. Cardillo[148], I. Carli[142], T. Carli[36], G. Carlino[68a], B. T. Carlson[138], L. Carminati[67a,67b], R. M. D. Carney[44a,44b], S. Caron[118], E. Carquin[146b], S. Carrá[67a,67b], J. W. S. Carter[166], M. P. Casado[14,f], A. F. Casha[166], D. W. Casper[170], R. Castelijn[119], F. L. Castillo[173], V. Castillo Gimenez[173], N. F. Castro[139a,139e], A. Catinaccio[36], J. R. Catmore[133], A. Cattai[36], J. Caudron[24], V. Cavaliere[29], E. Cavallaro[14], D. Cavalli[67a], M. Cavalli-Sforza[14], V. Cavasinni[70a,70b], E. Celebi[12b], F. Ceradini[73a,73b], L. Cerda Alberich[173], A. S. Cerqueira[79a], A. Cerri[155], L. Cerrito[72a,72b], F. Cerutti[18], A. Cervelli[23b,23a], S. A. Cetin[12b], A. Chafaq[35a], D. Chakraborty[120], S. K. Chan[58], W. S. Chan[119], W. Y. Chan[89], J. D. Chapman[32], B. Chargeishvili[158b], D. G. Charlton[21], C. C. Chau[34], C. A. Chavez Barajas[155], S. Che[125], A. Chegwidden[105], S. Chekanov[6], S. V. Chekulaev[167a], G. A. Chelkov[78,av], M. A. Chelstowska[36], B. Chen[77], C. Chen[59a], C. H. Chen[77], H. Chen[29], J. Chen[59a], J. Chen[39], S. Chen[136], S. J. Chen[15c], X. Chen[15b,au], Y. Chen[81], Y-H. Chen[45], H. C. Cheng[62a], H. J. Cheng[15a,15d], A. Cheplakov[78], E. Cheremushkina[122], R. Cherkaoui El Moursli[35e], E. Cheu[7], K. Cheung[63], T. J. A. Chevalérias[144], L. Chevalier[144], V. Chiarella[50], G. Chiarelli[70a], G. Chiodini[66a], A. S. Chisholm[36,21], A. Chitan[27b], I. Chiu[162], Y. H. Chiu[175], M. V. Chizhov[78], K. Choi[64], A. R. Chomont[131], S. Chouridou[161], Y. S. Chow[119], V. Christodoulou[93], M. C. Chu[62a], J. Chudoba[140], A. J. Chuinard[102], J. J. Chwastowski[83], L. Chytka[129], D. Cinca[46], V. Cindro[90], I. A. Cioară[27b], A. Ciocio[18], F. Cirotto[68a,68b], Z. H. Citron[179], M. Citterio[67a], B. M. Ciungu[166], A. Clark[53], M. R. Clark[39], P. J. Clark[49], C. Clement[44a,44b], Y. Coadou[100], M. Cobal[65a,65c], A. Coccaro[54b], J. Cochran[77], H. Cohen[160], A. E. C. Coimbra[179], L. Colasurdo[118], B. Cole[39], A. P. Colijn[119], J. Collot[57], P. Conde Muiño[139a,g], E. Coniavitis[51], S. H. Connell[33b], I. A. Connelly[99], S. Constantinescu[27b], F. Conventi[68a,ay], A. M. Cooper-Sarkar[134], F. Cormier[174], K. J. R. Cormier[166], L. D. Corpe[93], M. Corradi[71a,71b], E. E. Corrigan[95], F. Corriveau[102,ad], A. Cortes-Gonzalez[36], M. J. Costa[173], F. Costanza[5], D. Costanzo[148], G. Cowan[92], J. W. Cowley[32], J. Crane[99], K. Cranmer[123], S. J. Crawley[56], R. A. Creager[136], S. Crépé-Renaudin[57], F. Crescioli[135], M. Cristinziani[24], V. Croft[123], G. Crosetti[41b,41a], A. Cueto[97], T. Cuhadar Donszelmann[148], A. R. Cukierman[152], S. Czekierda[83], P. Czodrowski[36], M. J. Da Cunha Sargedas De Sousa[59b], C. Da Via[99], W. Dabrowski[82a], T. Dado[28a], S. Dahbi[35e], T. Dai[104], C. Dallapiccola[101], M. Dam[40], G. D'amen[23b,23a], J. Damp[98], J. R. Dandoy[136], M. F. Daneri[30], N. P. Dang[180], N. D. Dann[99], M. Danninger[174], V. Dao[36], G. Darbo[54b], O. Dartsi[5], A. Dattagupta[130], T. Daubney[45], S. D'Auria[67a,67b], W. Davey[24], C. David[45], T. Davidek[142], D. R. Davis[48], E. Dawe[103], I. Dawson[148], K. De[8], R. De Asmundis[68a], A. De Benedetti[127], M. De Beurs[119], S. De Castro[23b,23a], S. De Cecco[71a,71b], N. De Groot[118], P. de Jong[119], H. De la Torre[105], A. De Maria[70a,70b], D. De Pedis[71a], A. De Salvo[71a], U. De Sanctis[72a,72b], M. De Santis[72a,72b], A. De Santo[155], K. De Vasconcelos Corga[100], J. B. De Vivie De Regie[131], C. Debenedetti[145], D. V. Dedovich[78], A. M. Deiana[42], M. Del Gaudio[41b,41a], J. Del Peso[97], Y. Delabat Diaz[45], D. Delgove[131], F. Deliot[144], C. M. Delitzsch[7], M. Della Pietra[68a,68b], D. Della Volpe[53], A. Dell'Acqua[36], L. Dell'Asta[25], M. Delmastro[5], C. Delporte[131], P. A. Delsart[57], D. A. DeMarco[166], S. Demers[182], M. Demichev[78], S. P. Denisov[122], D. Denysiuk[119], L. D'Eramo[135], D. Derendarz[83], J. E. Derkaoui[35d], F. Derue[135], P. Dervan[89], K. Desch[24], C. Deterre[45], K. Dette[166], M. R. Devesa[30], P. O. Deviveiros[36], A. Dewhurst[143], S. Dhaliwal[26], F. A. Di Bello[53], A. Di Ciaccio[72a,72b], L. Di Ciaccio[5], W. K. Di Clemente[136], C. Di Donato[68a,68b], A. Di Girolamo[36], G. Di Gregorio[70a,70b], B. Di Micco[73a,73b], R. Di Nardo[101], K. F. Di Petrillo[58], R. Di Sipio[166], D. Di Valentino[34], C. Diaconu[100], F. A. Dias[40], T. Dias Do Vale[139a,139e], M. A. Diaz[146a], J. Dickinson[18], E. B. Diehl[104], J. Dietrich[19], S. Díez Cornell[45], A. Dimitrievska[18], J. Dingfelder[24], F. Dittus[36], F. Djama[100], T. Djobava[158b], J. I. Djuvsland[17], M. A. B. Do Vale[79c], M. Dobre[27b], D. Dodsworth[26], C. Doglioni[95], J. Dolejsi[142], Z. Dolezal[142], M. Donadelli[79d], J. Donini[38], A. D'onofrio[91], M. D'Onofrio[89], J. Dopke[143], A. Doria[68a], M. T. Dova[87], A. T. Doyle[56], E. Drechsler[151], E. Dreyer[151], T. Dreyer[52], Y. Du[59b], Y. Duan[59b], F. Dubinin[109], M. Dubovsky[28a], A. Dubreuil[53], E. Duchovni[179], G. Duckeck[113], A. Ducourthial[135], O. A. Ducu[108,x], D. Duda[114], A. Dudarev[36], A. C. Dudder[98], E. M. Duffield[18], L. Duflot[131], M. Dührssen[36], C. Dülsen[181], M. Dumancic[179], A. E. Dumitriu[27b], A. K. Duncan[56], M. Dunford[60a], A. Duperrin[100], H. Duran Yildiz[4a], M. Düren[55], A. Durglishvili[158b], D. Duschinger[47], B. Dutta[45], D. Duvnjak[1], G. I. Dyckes[136], M. Dyndal[45], S. Dysch[99], B. S. Dziedzic[83], K. M. Ecker[114], R. C. Edgar[104], T. Eifert[36], G. Eigen[17], K. Einsweiler[18], T. Ekelof[171], M. El Kacimi[35c], R. El Kosseifi[100], V. Ellajosyula[171], M. Ellert[171], F. Ellinghaus[181], A. A. Elliot[91], N. Ellis[36], J. Elmsheuser[29], M. Elsing[36], D. Emeliyanov[143], A. Emerman[39], Y. Enari[162], J. S. Ennis[177], M. B. Epland[48], J. Erdmann[46], A. Ereditato[20], M. Escalier[131], C. Escobar[173], O. Estrada Pastor[173],

A. I. Etienvre[144], E. Etzion[160], H. Evans[64], A. Ezhilov[137], M. Ezzi[35e], F. Fabbri[56], L. Fabbri[23b,23a], V. Fabiani[118], G. Facini[93], R. M. Faisca Rodrigues Pereira[139a], R. M. Fakhrutdinov[122], S. Falciano[71a], P. J. Falke[5], S. Falke[5], J. Faltova[142], Y. Fang[15a], Y. Fang[15a], M. Fanti[67a,67b], A. Farbin[8], A. Farilla[73a], E. M. Farina[69a,69b], T. Farooque[105], S. Farrell[18], S. M. Farrington[177], P. Farthouat[36], F. Fassi[35e], P. Fassnacht[36], D. Fassouliotis[9], M. Faucci Giannelli[49], W. J. Fawcett[32], L. Fayard[131], O. L. Fedin[137,p], W. Fedorko[174], M. Feickert[42], S. Feigl[133], L. Feligioni[100], C. Feng[59b], E. J. Feng[36], M. Feng[48], M. J. Fenton[56], A. B. Fenyuk[122], J. Ferrando[45], A. Ferrari[171], P. Ferrari[119], R. Ferrari[69a], D. E. Ferreira de Lima[60b], A. Ferrer[173], D. Ferrere[53], C. Ferretti[104], F. Fiedler[98], A. Filipčič[90], F. Filthaut[118], K. D. Finelli[25], M. C. N. Fiolhais[139a,139c,a], L. Fiorini[173], C. Fischer[14], W. C. Fisher[105], I. Fleck[150], P. Fleischmann[104], R. R. M. Fletcher[136], T. Flick[181], B. M. Flierl[113], L. F. Flores[136], L. R. Flores Castillo[62a], F. M. Follega[74a,74b], N. Fomin[17], G. T. Forcolin[74a,74b], A. Formica[144], F. A. Förster[14], A. C. Forti[99], A. G. Foster[21], D. Fournier[131], H. Fox[88], S. Fracchia[148], P. Francavilla[70a,70b], M. Franchini[23b,23a], S. Franchino[60a], D. Francis[36], L. Franconi[145], M. Franklin[58], M. Frate[170], A. N. Fray[91], D. Freeborn[93], B. Freund[108], W. S. Freund[79b], E. M. Freundlich[46], D. C. Frizzell[127], D. Froidevaux[36], J. A. Frost[134], C. Fukunaga[163], E. Fullana Torregrosa[173], E. Fumagalli[54b,54a], T. Fusayasu[115], J. Fuster[173], A. Gabrielli[23b,23a], A. Gabrielli[18], G. P. Gach[82a], S. Gadatsch[53], P. Gadow[114], G. Gagliardi[54b,54a], L. G. Gagnon[108], C. Galea[27b], B. Galhardo[139a,139c], E. J. Gallas[134], B. J. Gallop[143], P. Gallus[141], G. Galster[40], R. Gamboa Goni[91], K. K. Gan[125], S. Ganguly[179], J. Gao[59a], Y. Gao[89], Y. S. Gao[31,m], C. García[173], J. E. García Navarro[173], J. A. García Pascual[15a], C. Garcia-Argos[51], M. Garcia-Sciveres[18], R. W. Gardner[37], N. Garelli[152], S. Gargiulo[51], V. Garonne[133], A. Gaudiello[54b,54a], G. Gaudio[69a], I. L. Gavrilenko[109], A. Gavrilyuk[110], C. Gay[174], G. Gaycken[24], E. N. Gazis[10], C. N. P. Gee[143], J. Geisen[52], M. Geisen[98], M. P. Geisler[60a], C. Gemme[54b], M. H. Genest[57], C. Geng[104], S. Gentile[71a,71b], S. George[92], D. Gerbaudo[14], G. Gessner[46], S. Ghasemi[150], M. Ghasemi Bostanabad[175], M. Ghneimat[24], A. Ghosh[76], B. Giacobbe[23b], S. Giagu[71a,71b], N. Giangiacomi[23b,23a], P. Giannetti[70a], A. Giannini[68a,68b], S. M. Gibson[92], M. Gignac[145], D. Gillberg[34], G. Gilles[181], D. M. Gingrich[3,aw], M. P. Giordani[65a,65c], F. M. Giorgi[23b], P. F. Giraud[144], G. Giugliarelli[65a,65c], D. Giugni[67a], F. Giuli[134], M. Giulini[60b], S. Gkaitatzis[161], I. Gkialas[9,i], E. L. Gkougkousis[14], P. Gkountoumis[10], L. K. Gladilin[112], C. Glasman[97], J. Glatzer[14], P. C. F. Glaysher[45], A. Glazov[45], M. Goblirsch-Kolb[26], S. Goldfarb[103], T. Golling[53], D. Golubkov[122], A. Gomes[139a,139b], R. Goncalves Gama[52], R. Gonçalo[139a,139b], G. Gonella[51], L. Gonella[21], A. Gongadze[78], F. Gonnella[21], J. L. Gonski[58], S. González de la Hoz[173], S. Gonzalez-Sevilla[53], L. Goossens[36], P. A. Gorbounov[110], H. A. Gordon[29], B. Gorini[36], E. Gorini[66a,66b], A. Gorišek[90], A. T. Goshaw[48], C. Gössling[46], M. I. Gostkin[78], C. A. Gottardo[24], C. R. Goudet[131], D. Goujdami[35c], A. G. Goussiou[147], N. Govender[33b,b], C. Goy[5], E. Gozani[159], I. Grabowska-Bold[82a], P. O. J. Gradin[171], E. C. Graham[89], J. Gramling[170], E. Gramstad[133], S. Grancagnolo[19], M. Grandi[155], V. Gratchev[137], P. M. Gravila[27f], F. G. Gravili[66a,66b], C. Gray[56], H. M. Gray[18], C. Grefe[24], K. Gregersen[95], I. M. Gregor[45], P. Grenier[152], K. Grevtsov[45], N. A. Grieser[127], J. Griffiths[8], A. A. Grillo[145], K. Grimm[31,l], S. Grinstein[14,y], J.-F. Grivaz[131], S. Groh[98], E. Gross[179], J. Grosse-Knetter[52], Z. J. Grout[93], C. Grud[104], A. Grummer[117], L. Guan[104], W. Guan[180], J. Guenther[36], A. Guerguichon[131], F. Guescini[167a], D. Guest[170], R. Gugel[51], B. Gui[125], T. Guillemin[5], S. Guindon[36], U. Gul[56], J. Guo[59c], W. Guo[104], Y. Guo[59a,s], Z. Guo[100], R. Gupta[45], S. Gurbuz[12c], G. Gustavino[127], P. Gutierrez[127], C. Gutschow[93], C. Guyot[144], M. P. Guzik[82a], C. Gwenlan[134], C. B. Gwilliam[89], A. Haas[123], C. Haber[18], H. K. Hadavand[8], N. Haddad[35e], A. Hadef[59a], S. Hageböck[36], M. Hagihara[168], M. Haleem[176], J. Haley[128], G. Halladjian[105], G. D. Hallewell[100], K. Hamacher[181], P. Hamal[129], K. Hamano[175], H. Hamdaoui[35e], G. N. Hamity[148], K. Han[59a,ak], L. Han[59a], S. Han[15a,15d], K. Hanagaki[80,v], M. Hance[145], D. M. Handl[113], B. Haney[136], R. Hankache[135], P. Hanke[60a], E. Hansen[95], J. B. Hansen[40], J. D. Hansen[40], M. C. Hansen[24], P. H. Hansen[40], E. C. Hanson[99], K. Hara[168], A. S. Hard[180], T. Harenberg[181], S. Harkusha[106], P. F. Harrison[177], N. M. Hartmann[113], Y. Hasegawa[149], A. Hasib[49], S. Hassani[144], S. Haug[20], R. Hauser[105], L. Hauswald[47], L. B. Havener[39], M. Havranek[141], C. M. Hawkes[21], R. J. Hawkings[36], D. Hayden[105], C. Hayes[154], C. P. Hays[134], J. M. Hays[91], H. S. Hayward[89], S. J. Haywood[143], F. He[59a], M. P. Heath[49], V. Hedberg[95], L. Heelan[8], S. Heer[24], K. K. Heidegger[51], J. Heilman[34], S. Heim[45], T. Heim[18], B. Heinemann[45,ar], J. J. Heinrich[113], L. Heinrich[123], C. Heinz[55], J. Hejbal[140], L. Helary[60b], A. Held[174], S. Hellesund[133], C. M. Helling[145], S. Hellman[44a,44b], C. Helsens[36], R. C. W. Henderson[88], Y. Heng[180], S. Henkelmann[174], A. M. Henriques Correia[36], G. H. Herbert[19], H. Herde[26], V. Herget[176], Y. Hernández Jiménez[33c], H. Herr[98], M. G. Herrmann[113], T. Herrmann[47], G. Herten[51], R. Hertenberger[113], L. Hervas[36], T. C. Herwig[136], G. G. Hesketh[93], N. P. Hessey[167a], A. Higashida[162], S. Higashino[80], E. Higón-Rodriguez[173], K. Hildebrand[37], E. Hill[175], J. C. Hill[32], K. K. Hill[29], K. H. Hiller[45], S. J. Hillier[21], M. Hils[47], I. Hinchliffe[18], F. Hinterkeuser[24], M. Hirose[132], D. Hirschbuehl[181], B. Hiti[90], O. Hladik[140], D. R. Hlaluku[33c], X. Hoad[49], J. Hobbs[154], N. Hod[179], M. C. Hodgkinson[148], A. Hoecker[36], F. Hoenig[113], D. Hohn[51], D. Hohov[131], T. R. Holmes[37], M. Holzbock[113], M. Homann[46], L. B. A. H Hommels[32], S. Honda[168], T. Honda[80], T. M. Hong[138], A. Hönle[114], B. H. Hooberman[172], W. H. Hopkins[6], Y. Horii[116], P. Horn[47], A. J. Horton[151], L. A. Horyn[37], J-Y. Hostachy[57], A. Hostiuc[147], S. Hou[157], A. Hoummada[35a], J. Howarth[99], J. Hoya[87], M. Hrabovsky[129], J. Hrdinka[36], I. Hristova[19], J. Hrivnac[131], A. Hrynevich[107],

T. Hryn'ova[5], P. J. Hsu[63], S.-C. Hsu[147], Q. Hu[29], S. Hu[59c], Y. Huang[15a], Z. Hubacek[141], F. Hubaut[100], M. Huebner[24], F. Huegging[24], T. B. Huffman[134], M. Huhtinen[36], R. F. H. Hunter[34], P. Huo[154], A. M. Hupe[34], N. Huseynov[78,af], J. Huston[105], J. Huth[58], R. Hyneman[104], G. Iacobucci[53], G. Iakovidis[29], I. Ibragimov[150], L. Iconomidou-Fayard[131], Z. Idrissi[35e], P. I. Iengo[36], R. Ignazzi[40], O. Igonkina[119,aa,*], R. Iguchi[162], T. Iizawa[53], Y. Ikegami[80], M. Ikeno[80], D. Iliadis[161], N. Ilic[118], F. Iltzsche[47], G. Introzzi[69a,69b], M. Iodice[73a], K. Iordanidou[39], V. Ippolito[71a,71b], M. F. Isacson[171], N. Ishijima[132], M. Ishino[162], M. Ishitsuka[164], W. Islam[128], C. Issever[134], S. Istin[159], F. Ito[168], J. M. Iturbe Ponce[62a], R. Iuppa[74a,74b], A. Ivina[179], H. Iwasaki[80], J. M. Izen[43], V. Izzo[68a], P. Jacka[140], P. Jackson[1], R. M. Jacobs[24], V. Jain[2], G. Jäkel[181], K. B. Jakobi[98], K. Jakobs[51], S. Jakobsen[75], T. Jakoubek[140], D. O. Jamin[128], R. Jansky[53], J. Janssen[24], M. Janus[52], P. A. Janus[82a], G. Jarlskog[95], N. Javadov[78,af], T. Javůrek[36], M. Javurkova[51], F. Jeanneau[144], L. Jeanty[130], J. Jejelava[158a,ag], A. Jelinskas[177], P. Jenni[51,c], J. Jeong[45], N. Jeong[45], S. Jézéquel[5], H. Ji[180], J. Jia[154], H. Jiang[77], Y. Jiang[59a], Z. Jiang[152,q], S. Jiggins[51], F. A. Jimenez Morales[38], J. Jimenez Pena[173], S. Jin[15c], A. Jinaru[27b], O. Jinnouchi[164], H. Jivan[33c], P. Johansson[148], K. A. Johns[7], C. A. Johnson[64], K. Jon-And[44a,44b], R. W. L. Jones[88], S. D. Jones[155], S. Jones[7], T. J. Jones[89], J. Jongmanns[60a], P. M. Jorge[139a,139b], J. Jovicevic[167a], X. Ju[18], J. J. Junggeburth[114], A. Juste Rozas[14,y], A. Kaczmarska[83], M. Kado[131], H. Kagan[125], M. Kagan[152], T. Kaji[178], E. Kajomovitz[159], C. W. Kalderon[95], A. Kaluza[98], A. Kamenshchikov[122], L. Kanjir[90], Y. Kano[162], V. A. Kantserov[111], J. Kanzaki[80], L. S. Kaplan[180], D. Kar[33c], M. J. Kareem[167b], E. Karentzos[10], S. N. Karpov[78], Z. M. Karpova[78], V. Kartvelishvili[88], A. N. Karyukhin[122], L. Kashif[180], R. D. Kass[125], A. Kastanas[44a,44b], Y. Kataoka[162], C. Kato[59d,59c], J. Katzy[45], K. Kawade[81], K. Kawagoe[86], T. Kawaguchi[116], T. Kawamoto[162], G. Kawamura[52], E. F. Kay[89], V. F. Kazanin[121b,121a], R. Keeler[175], R. Kehoe[42], J. S. Keller[34], E. Kellermann[95], J. J. Kempster[21], J. Kendrick[21], O. Kepka[140], S. Kersten[181], B. P. Kerševan[90], S. Ketabchi Haghighat[166], R. A. Keyes[102], M. Khader[172], F. Khalil-Zada[13], A. Khanov[128], A. G. Kharlamov[121b,121a], T. Kharlamova[121b,121a], E. E. Khoda[174], A. Khodinov[165], T. J. Khoo[53], E. Khramov[78], J. Khubua[158b], S. Kido[81], M. Kiehn[53], C. R. Kilby[92], Y. K. Kim[37], N. Kimura[65a,65c], O. M. Kind[19], B. T. King[89,*], D. Kirchmeier[47], J. Kirk[143], A. E. Kiryunin[114], T. Kishimoto[162], V. Kitali[45], O. Kivernyk[5], E. Kladiva[28b,*], T. Klapdor-Kleingrothaus[51], M. H. Klein[104], M. Klein[89], U. Klein[89], K. Kleinknecht[98], P. Klimek[120], A. Klimentov[29], T. Klingl[24], T. Klioutchnikova[36], F. F. Klitzner[113], P. Kluit[119], S. Kluth[114], E. Kneringer[75], E. B. F. G. Knoops[100], A. Knue[51], D. Kobayashi[86], T. Kobayashi[162], M. Kobel[47], M. Kocian[152], P. Kodys[142], P. T. Koenig[24], T. Koffas[34], N. M. Köhler[114], T. Koi[152], M. Kolb[60b], I. Koletsou[5], T. Kondo[80], N. Kondrashova[59c], K. Köneke[51], A. C. König[118], T. Kono[124], R. Konoplich[123,an], V. Konstantinides[93], N. Konstantinidis[93], B. Konya[95], R. Kopeliansky[64], S. Koperny[82a], K. Korcyl[83], K. Kordas[161], G. Koren[160], A. Korn[93], I. Korolkov[14], E. V. Korolkova[148], N. Korotkova[112], O. Kortner[114], S. Kortner[114], T. Kosek[142], V. V. Kostyukhin[24], A. Kotwal[48], A. Koulouris[10], A. Kourkoumeli-Charalampidi[69a,69b], C. Kourkoumelis[9], E. Kourlitis[148], V. Kouskoura[29], A. B. Kowalewska[83], R. Kowalewski[175], C. Kozakai[162], W. Kozanecki[144], A. S. Kozhin[122], V. A. Kramarenko[112], G. Kramberger[90], D. Krasnopevtsev[59a], M. W. Krasny[135], A. Krasznahorkay[36], D. Krauss[114], J. A. Kremer[82a], J. Kretzschmar[89], P. Krieger[166], K. Krizka[18], K. Kroeninger[46], H. Kroha[114], J. Kroll[140], J. Kroll[136], J. Krstic[16], U. Kruchonak[78], H. Krüger[24], N. Krumnack[77], M. C. Kruse[48], T. Kubota[103], S. Kuday[4b], J. T. Kuechler[45], S. Kuehn[36], A. Kugel[60a], T. Kuhl[45], V. Kukhtin[78], R. Kukla[100], Y. Kulchitsky[106,aj], S. Kuleshov[146b], Y. P. Kulinich[172], M. Kuna[57], T. Kunigo[84], A. Kupco[140], T. Kupfer[46], O. Kuprash[51], H. Kurashige[81], L. L. Kurchaninov[167a], Y. A. Kurochkin[106], A. Kurova[111], M. G. Kurth[15a,15d], E. S. Kuwertz[36], M. Kuze[164], J. Kvita[129], T. Kwan[102], A. La Rosa[114], J. L. La Rosa Navarro[79d], L. La Rotonda[41b,41a], F. La Ruffa[41b,41a], C. Lacasta[173], F. Lacava[71a,71b], J. Lacey[45], D. P. J. Lack[99], H. Lacker[19], D. Lacour[135], E. Ladygin[78], R. Lafaye[5], B. Laforge[135], T. Lagouri[33c], S. Lai[52], S. Lammers[64], W. Lampl[7], E. Lançon[29], U. Landgraf[51], M. P. J. Landon[91], M. C. Lanfermann[53], V. S. Lang[45], J. C. Lange[52], R. J. Langenberg[36], A. J. Lankford[170], F. Lanni[29], K. Lantzsch[24], A. Lanza[69a], A. Lapertosa[54b,54a], S. Laplace[135], J. F. Laporte[144], T. Lari[67a], F. Lasagni Manghi[23b,23a], M. Lassnig[36], T. S. Lau[62a], A. Laudrain[131], A. Laurier[34], M. Lavorgna[68a,68b], M. Lazzaroni[67a,67b], B. Le[103], O. Le Dortz[135], E. Le Guirriec[100], E. P. Le Quilleuc[144], M. LeBlanc[7], T. LeCompte[6], F. Ledroit-Guillon[57], C. A. Lee[29], G. R. Lee[146a], L. Lee[58], S. C. Lee[157], S. J. Lee[34], B. Lefebvre[102], M. Lefebvre[175], F. Legger[113], C. Leggett[18], K. Lehmann[151], N. Lehmann[181], G. Lehmann Miotto[36], W. A. Leight[45], A. Leisos[161,w], M. A. L. Leite[79d], R. Leitner[142], D. Lellouch[179,*], K. J. C. Leney[93], T. Lenz[24], B. Lenzi[36], R. Leone[7], S. Leone[70a], C. Leonidopoulos[49], A. Leopold[135], G. Lerner[155], C. Leroy[108], R. Les[166], A. A. J. Lesage[144], C. G. Lester[32], M. Levchenko[137], J. Levêque[5], D. Levin[104], L. J. Levinson[179], B. Li[15b], B. Li[104], C-Q. Li[59a,am], H. Li[59a], H. Li[59b], K. Li[152], L. Li[59c], M. Li[15a], Q. Li[15a,15d], Q. Y. Li[59a], S. Li[59d,59c], X. Li[59c], Y. Li[45], Z. Liang[15a], B. Liberti[72a], A. Liblong[166], K. Lie[62c], S. Liem[119], A. Limosani[156], C. Y. Lin[32], K. Lin[105], T. H. Lin[98], R. A. Linck[64], J. H. Lindon[21], A. L. Lionti[53], E. Lipeles[136], A. Lipniacka[17], M. Lisovyi[60b], T. M. Liss[172,at], A. Lister[174], A. M. Litke[145], J. D. Little[8], B. Liu[77], B. L. Liu[6], H. B. Liu[29], H. Liu[104], J. B. Liu[59a], J. K. K. Liu[134], K. Liu[135], M. Liu[59a], P. Liu[18], Y. Liu[15a,15d], Y. L. Liu[59a], Y. W. Liu[59a], M. Livan[69a,69b], A. Lleres[57], J. Llorente Merino[15a], S. L. Lloyd[91], C. Y. Lo[62b], F. Lo Sterzo[42], E. M. Lobodzinska[45],

P. Loch[7], T. Lohse[19], K. Lohwasser[148], M. Lokajicek[140], J. D. Long[172], R. E. Long[88], L. Longo[66a,66b], K. A. Looper[125], J. A. Lopez[146b], I. Lopez Paz[99], A. Lopez Solis[148], J. Lorenz[113], N. Lorenzo Martinez[5], M. Losada[22], P. J. Lösel[113], A. Lösle[51], X. Lou[45], X. Lou[15a], A. Lounis[131], J. Love[6], P. A. Love[88], J. J. Lozano Bahilo[173], H. Lu[62a], M. Lu[59a], Y. J. Lu[63], H. J. Lubatti[147], C. Luci[71a,71b], A. Lucotte[57], C. Luedtke[51], F. Luehring[64], I. Luise[135], L. Luminari[71a], B. Lund-Jensen[153], M. S. Lutz[101], P. M. Luzi[135], D. Lynn[29], R. Lysak[140], E. Lytken[95], F. Lyu[15a], V. Lyubushkin[78], T. Lyubushkina[78], H. Ma[29], L. L. Ma[59b], Y. Ma[59b], G. Maccarrone[50], A. Macchiolo[114], C. M. Macdonald[148], J. Machado Miguens[136,139b], D. Madaffari[173], R. Madar[38], W. F. Mader[47], N. Madysa[47], J. Maeda[81], K. Maekawa[162], S. Maeland[17], T. Maeno[29], M. Maerker[47], A. S. Maevskiy[112], V. Magerl[51], D. J. Mahon[39], C. Maidantchik[79b], T. Maier[113], A. Maio[139a,139b,139d], O. Majersky[28a], S. Majewski[130], Y. Makida[80], N. Makovec[131], B. Malaescu[135], Pa. Malecki[83], V. P. Maleev[137], F. Malek[57], U. Mallik[76], D. Malon[6], C. Malone[32], S. Maltezos[10], S. Malyukov[36], J. Mamuzic[173], G. Mancini[50], I. Mandić[90], L. Manhaes de Andrade Filho[79a], I. M. Maniatis[161], J. Manjarres Ramos[47], K. H. Mankinen[95], A. Mann[113], A. Manousos[75], B. Mansoulie[144], S. Manzoni[119], A. Marantis[161], G. Marceca[30], L. Marchese[134], G. Marchiori[135], M. Marcisovsky[140], C. Marcon[95], C. A. Marin Tobon[36], M. Marjanovic[38], F. Marroquim[79b], Z. Marshall[18], M. U. F Martensson[171], S. Marti-Garcia[173], C. B. Martin[125], T. A. Martin[177], V. J. Martin[49], B. Martin dit Latour[17], M. Martinez[14,y], V. I. Martinez Outschoorn[101], S. Martin-Haugh[143], V. S. Martoiu[27b], A. C. Martyniuk[93], A. Marzin[36], L. Masetti[98], T. Mashimo[162], R. Mashinistov[109], J. Masik[99], A. L. Maslennikov[121b,121a], L. H. Mason[103], L. Massa[72a,72b], P. Massarotti[68a,68b], P. Mastrandrea[70a,70b], A. Mastroberardino[41b,41a], T. Masubuchi[162], P. Mättig[24], J. Maurer[27b], B. Maček[90], S. J. Maxfield[89], D. A. Maximov[121b,121a], R. Mazini[157], I. Maznas[161], S. M. Mazza[145], S. P. Mc Kee[104], T. G. McCarthy[114], L. I. McClymont[93], W. P. McCormack[18], E. F. McDonald[103], J. A. Mcfayden[36], M. A. McKay[42], K. D. McLean[175], S. J. McMahon[143], P. C. McNamara[103], C. J. McNicol[177], R. A. McPherson[175,ad], J. E. Mdhluli[33c], Z. A. Meadows[101], S. Meehan[147], T. Megy[51], S. Mehlhase[113], A. Mehta[89], T. Meideck[57], B. Meirose[43], D. Melini[173,ax], B. R. Mellado Garcia[33c], J. D. Mellenthin[52], M. Melo[28a], F. Meloni[45], A. Melzer[24], S. B. Menary[99], E. D. Mendes Gouveia[139a,139e], L. Meng[36], X. T. Meng[104], S. Menke[114], E. Meoni[41b,41a], S. Mergelmeyer[19], S. A. M. Merkt[138], C. Merlassino[20], P. Mermod[53], L. Merola[68a,68b], C. Meroni[67a], J. K. R. Meshreki[150], A. Messina[71a,71b], J. Metcalfe[6], A. S. Mete[170], C. Meyer[64], J. Meyer[159], J-P. Meyer[144], H. Meyer Zu Theenhausen[60a], F. Miano[155], R. P. Middleton[143], L. Mijović[49], G. Mikenberg[179], M. Mikestikova[140], M. Mikuž[90], M. Milesi[103], A. Milic[166], D. A. Millar[91], D. W. Miller[37], A. Milov[179], D. A. Milstead[44a,44b], R. A. Mina[152,q], A. A. Minaenko[122], M. Miñano Moya[173], I. A. Minashvili[158b], A. I. Mincer[123], B. Mindur[82a], M. Mineev[78], Y. Minegishi[162], Y. Ming[180], L. M. Mir[14], A. Mirto[66a,66b], K. P. Mistry[136], T. Mitani[178], J. Mitrevski[113], V. A. Mitsou[173], M. Mittal[59c], A. Miucci[20], P. S. Miyagawa[148], A. Mizukami[80], J. U. Mjörnmark[95], T. Mkrtchyan[183], M. Mlynarikova[142], T. Moa[44a,44b], K. Mochizuki[108], P. Mogg[51], S. Mohapatra[39], R. Moles-Valls[24], M. C. Mondragon[105], K. Mönig[45], J. Monk[40], E. Monnier[100], A. Montalbano[151], J. Montejo Berlingen[36], F. Monticelli[87], S. Monzani[67a], N. Morange[131], D. Moreno[22], M. Moreno Llácer[36], P. Morettini[54b], M. Morgenstern[119], S. Morgenstern[47], D. Mori[151], M. Morii[58], M. Morinaga[178], V. Morisbak[133], A. K. Morley[36], G. Mornacchi[36], A. P. Morris[93], L. Morvaj[154], P. Moschovakos[10], M. Mosidze[158b], H. J. Moss[148], J. Moss[31,n], K. Motohashi[164], E. Mountricha[36], E. J. W. Moyse[101], S. Muanza[100], F. Mueller[114], J. Mueller[138], R. S. P. Mueller[113], D. Muenstermann[88], G. A. Mullier[95], F. J. Munoz Sanchez[99], P. Murin[28b], W. J. Murray[177,143], A. Murrone[67a,67b], M. Muškinja[90], C. Mwewa[33a], A. G. Myagkov[122,ao], J. Myers[130], M. Myska[141], B. P. Nachman[18], O. Nackenhorst[46], K. Nagai[134], K. Nagano[80], Y. Nagasaka[61], M. Nagel[51], E. Nagy[100], A. M. Nairz[36], Y. Nakahama[116], K. Nakamura[80], T. Nakamura[162], I. Nakano[126], H. Nanjo[132], F. Napolitano[60a], R. F. Naranjo Garcia[45], R. Narayan[11], D. I. Narrias Villar[60a], I. Naryshkin[137], T. Naumann[45], G. Navarro[22], H. A. Neal[104,*], P. Y. Nechaeva[109], F. Nechansky[45], T. J. Neep[144], A. Negri[69a,69b], M. Negrini[23b], S. Nektarijevic[118], C. Nellist[52], M. E. Nelson[134], S. Nemecek[140], P. Nemethy[123], M. Nessi[36,e], M. S. Neubauer[172], M. Neumann[181], P. R. Newman[21], T. Y. Ng[62c], Y. S. Ng[19], Y. W. Y. Ng[170], H. D. N. Nguyen[100], T. Nguyen Manh[108], E. Nibigira[38], R. B. Nickerson[134], R. Nicolaidou[144], D. S. Nielsen[40], J. Nielsen[145], N. Nikiforou[11], V. Nikolaenko[122,ao], I. Nikolic-Audit[135], K. Nikolopoulos[21], P. Nilsson[29], H. R. Nindhito[53], Y. Ninomiya[80], A. Nisati[71a], N. Nishu[59c], R. Nisius[114], I. Nitsche[46], T. Nitta[178], T. Nobe[162], Y. Noguchi[84], M. Nomachi[132], I. Nomidis[135], M. A. Nomura[29], M. Nordberg[36], N. Norjoharuddeen[134], T. Novak[90], O. Novgorodova[47], R. Novotny[141], L. Nozka[129], K. Ntekas[170], E. Nurse[93], F. Nuti[103], F. G. Oakham[34,aw], H. Oberlack[114], J. Ocariz[135], A. Ochi[81], I. Ochoa[39], J. P. Ochoa-Ricoux[146a], K. O'Connor[26], S. Oda[86], S. Odaka[80], S. Oerdek[52], A. Ogrodnik[82a], A. Oh[99], S. H. Oh[48], C. C. Ohm[153], H. Oide[54b,54a], M. L. Ojeda[166], H. Okawa[168], Y. Okazaki[84], Y. Okumura[162], T. Okuyama[80], A. Olariu[27b], L. F. Oleiro Seabra[139a], S. A. Olivares Pino[146a], D. Oliveira Damazio[29], J. L. Oliver[1], M. J. R. Olsson[37], A. Olszewski[83], J. Olszowska[83], D. C. O'Neil[151], A. Onofre[139a,139e], K. Onogi[116], P. U. E. Onyisi[11], H. Oppen[133], M. J. Oreglia[37], G. E. Orellana[87], Y. Oren[160], D. Orestano[73a,73b], N. Orlando[14], A. A. O'Rourke[45], R. S. Orr[166], B. Osculati[54b,54a,*], V. O'Shea[56], R. Ospanov[59a], G. Otero y Garzon[30], H. Otono[86],

M. Ouchrif[35d], F. Ould-Saada[133], A. Ouraou[144], Q. Ouyang[15a], M. Owen[56], R. E. Owen[21], V. E. Ozcan[12c], N. Ozturk[8], J. Pacalt[129], H. A. Pacey[32], K. Pachal[151], A. Pacheco Pages[14], L. Pacheco Rodriguez[144], C. Padilla Aranda[14], S. Pagan Griso[18], M. Paganini[182], G. Palacino[64], S. Palazzo[49], S. Palestini[36], M. Palka[82b], D. Pallin[38], I. Panagoulias[10], C. E. Pandini[36], J. G. Panduro Vazquez[92], P. Pani[45], G. Panizzo[65a,65c], L. Paolozzi[53], K. Papageorgiou[9,i], A. Paramonov[6], D. Paredes Hernandez[62b], S. R. Paredes Saenz[134], B. Parida[165], T. H. Park[166], A. J. Parker[88], M. A. Parker[32], F. Parodi[54b,54a], E. W. P. Parrish[120], J. A. Parsons[39], U. Parzefall[51], L. Pascual Dominguez[135], V. R. Pascuzzi[166], J. M. P. Pasner[145], E. Pasqualucci[71a], S. Passaggio[54b], F. Pastore[92], P. Pasuwan[44a,44b], S. Pataraia[98], J. R. Pater[99], A. Pathak[180], T. Pauly[36], B. Pearson[114], M. Pedersen[133], L. Pedraza Diaz[118], R. Pedro[139a,139b], S. V. Peleganchuk[121b,121a], O. Penc[140], C. Peng[15a], H. Peng[59a], B. S. Peralva[79a], M. M. Perego[131], A. P. Pereira Peixoto[139a,139e], D. V. Perepelitsa[29], F. Peri[19], L. Perini[67a,67b], H. Pernegger[36], S. Perrella[68a,68b], V. D. Peshekhonov[78,*], K. Peters[45], R. F. Y. Peters[99], B. A. Petersen[36], T. C. Petersen[40], E. Petit[57], A. Petridis[1], C. Petridou[161], P. Petroff[131], M. Petrov[134], F. Petrucci[73a,73b], M. Pettee[182], N. E. Pettersson[101], A. Peyaud[144], R. Pezoa[146b], T. Pham[103], F. H. Phillips[105], P. W. Phillips[143], M. W. Phipps[172], G. Piacquadio[154], E. Pianori[18], A. Picazio[101], R. H. Pickles[99], R. Piegaia[30], J. E. Pilcher[37], A. D. Pilkington[99], M. Pinamonti[72a,72b], J. L. Pinfold[3], M. Pitt[179], L. Pizzimento[72a,72b], M.-A. Pleier[29], V. Pleskot[142], E. Plotnikova[78], D. Pluth[77], P. Podberezko[121b,121a], R. Poettgen[95], R. Poggi[53], L. Poggioli[131], I. Pogrebnyak[105], D. Pohl[24], I. Pokharel[52], G. Polesello[69a], A. Poley[18], A. Policicchio[71a,71b], R. Polifka[36], A. Polini[23b], C. S. Pollard[45], V. Polychronakos[29], D. Ponomarenko[111], L. Pontecorvo[36], G. A. Popeneciu[27d], D. M. Portillo Quintero[135], S. Pospisil[141], K. Potamianos[45], I. N. Potrap[78], C. J. Potter[32], H. Potti[11], T. Poulsen[95], J. Poveda[36], T. D. Powell[148], M. E. Pozo Astigarraga[36], P. Pralavorio[100], S. Prell[77], D. Price[99], M. Primavera[66a], S. Prince[102], M. L. Proffitt[147], N. Proklova[111], K. Prokofiev[62c], F. Prokoshin[146b], S. Protopopescu[29], J. Proudfoot[6], M. Przybycien[82a], A. Puri[172], P. Puzo[131], J. Qian[104], Y. Qin[99], A. Quadt[52], M. Queitsch-Maitland[45], A. Qureshi[1], P. Rados[103], F. Ragusa[67a,67b], G. Rahal[96], J. A. Raine[53], S. Rajagopalan[29], A. Ramirez Morales[91], K. Ran[15a,15d], T. Rashid[131], S. Raspopov[5], M. G. Ratti[67a,67b], D. M. Rauch[45], F. Rauscher[113], S. Rave[98], B. Ravina[148], I. Ravinovich[179], J. H. Rawling[99], M. Raymond[36], A. L. Read[133], N. P. Readioff[57], M. Reale[66a,66b], D. M. Rebuzzi[69a,69b], A. Redelbach[176], G. Redlinger[29], R. G. Reed[33c], K. Reeves[43], L. Rehnisch[19], J. Reichert[136], D. Reikher[160], A. Reiss[98], A. Rej[150], C. Rembser[36], H. Ren[15a], M. Rescigno[71a], S. Resconi[67a], E. D. Resseguie[136], S. Rettie[174], E. Reynolds[21], O. L. Rezanova[121b,121a], P. Reznicek[142], E. Ricci[74a,74b], R. Richter[114], S. Richter[45], E. Richter-Was[82b], O. Ricken[24], M. Ridel[135], P. Rieck[114], C. J. Riegel[181], O. Rifki[45], M. Rijssenbeek[154], A. Rimoldi[69a,69b], M. Rimoldi[20], L. Rinaldi[23b], G. Ripellino[153], B. Ristić[88], E. Ritsch[36], I. Riu[14], J. C. Rivera Vergara[146a], F. Rizatdinova[128], E. Rizvi[91], C. Rizzi[14], R. T. Roberts[99], S. H. Robertson[102,ad], D. Robinson[32], J. E. M. Robinson[45], A. Robson[56], E. Rocco[98], C. Roda[70a,70b], Y. Rodina[100], S. Rodriguez Bosca[173], A. Rodriguez Perez[14], D. Rodriguez Rodriguez[173], A. M. Rodríguez Vera[167b], S. Roe[36], O. Røhne[133], R. Röhrig[114], C. P. A. Roland[64], J. Roloff[58], A. Romaniouk[111], M. Romano[23b,23a], N. Rompotis[89], M. Ronzani[123], L. Roos[135], S. Rosati[71a], K. Rosbach[51], N-A. Rosien[52], B. J. Rosser[136], E. Rossi[45], E. Rossi[73a,73b], E. Rossi[68a,68b], L. P. Rossi[54b], L. Rossini[67a,67b], J. H. N. Rosten[32], R. Rosten[14], M. Rotaru[27b], J. Rothberg[147], D. Rousseau[131], D. Roy[33c], A. Rozanov[100], Y. Rozen[159], X. Ruan[33c], F. Rubbo[152], F. Rühr[51], A. Ruiz-Martinez[173], Z. Rurikova[51], N. A. Rusakovich[78], H. L. Russell[102], J. P. Rutherfoord[7], E. M. Rüttinger[45,k], Y. F. Ryabov[137], M. Rybar[39], G. Rybkin[131], S. Ryu[6], A. Ryzhov[122], G. F. Rzehorz[52], P. Sabatini[52], G. Sabato[119], S. Sacerdoti[131], H.F-W. Sadrozinski[145], R. Sadykov[78], F. Safai Tehrani[71a], P. Saha[120], M. Sahinsoy[60a], A. Sahu[181], M. Saimpert[45], M. Saito[162], T. Saito[162], H. Sakamoto[162], A. Sakharov[123,an], D. Salamani[53], G. Salamanna[73a,73b], J. E. Salazar Loyola[146b], P. H. Sales De Bruin[171], D. Salihagic[114,*], A. Salnikov[152], J. Salt[173], D. Salvatore[41b,41a], F. Salvatore[155], A. Salvucci[62a,62b,62c], A. Salzburger[36], J. Samarati[36], D. Sammel[51], D. Sampsonidis[161], D. Sampsonidou[161], J. Sánchez[173], A. Sanchez Pineda[65a,65c], H. Sandaker[133], C. O. Sander[45], M. Sandhoff[181], C. Sandoval[22], D. P. C. Sankey[143], M. Sannino[54b,54a], Y. Sano[116], A. Sansoni[50], C. Santoni[38], H. Santos[139a,139b], S. N. Santpur[18], A. Santra[173], A. Sapronov[78], J. G. Saraiva[139a,139d], O. Sasaki[80], K. Sato[168], E. Sauvan[5], P. Savard[166,aw], N. Savic[114], R. Sawada[162], C. Sawyer[143], L. Sawyer[94,al], C. Sbarra[23b], A. Sbrizzi[23a], T. Scanlon[93], J. Schaarschmidt[147], P. Schacht[114], B. M. Schachtner[113], D. Schaefer[37], L. Schaefer[136], J. Schaeffer[98], S. Schaepe[36], U. Schäfer[98], A. C. Schaffer[131], D. Schaile[113], R. D. Schamberger[154], N. Scharmberg[99], V. A. Schegelsky[137], D. Scheirich[142], F. Schenck[19], M. Schernau[170], C. Schiavi[54b,54a], S. Schier[145], L. K. Schildgen[24], Z. M. Schillaci[26], E. J. Schioppa[36], M. Schioppa[41b,41a], K. E. Schleicher[51], S. Schlenker[36], K. R. Schmidt-Sommerfeld[114], K. Schmieden[36], C. Schmitt[98], S. Schmitt[45], S. Schmitz[98], J. C. Schmoeckel[45], U. Schnoor[51], L. Schoeffel[144], A. Schoening[60b], E. Schopf[134], M. Schott[98], J. F. P. Schouwenberg[118], J. Schovancova[36], S. Schramm[53], A. Schulte[98], H-C. Schultz-Coulon[60a], M. Schumacher[51], B. A. Schumm[145], Ph. Schune[144], A. Schwartzman[152], T. A. Schwarz[104], Ph. Schwemling[144], R. Schwienhorst[105], A. Sciandra[24], G. Sciolla[26], M. Scornajenghi[41b,41a], F. Scuri[70a], F. Scutti[103], L. M. Scyboz[114], C. D. Sebastiani[71a,71b], P. Seema[19], S. C. Seidel[117], A. Seiden[145], T. Seiss[37], J. M. Seixas[79b], G. Sekhniaidze[68a], K. Sekhon[104], S. J. Sekula[42],

N. Semprini-Cesari[23b,23a], S. Sen[48], S. Senkin[38], C. Serfon[133], L. Serin[131], L. Serkin[65a,65b], M. Sessa[59a], H. Severini[127], F. Sforza[169], A. Sfyrla[53], E. Shabalina[52], J. D. Shahinian[145], N. W. Shaikh[44a,44b], D. Shaked Renous[179], L. Y. Shan[15a], R. Shang[172], J. T. Shank[25], M. Shapiro[18], A. Sharma[134], A. S. Sharma[1], P. B. Shatalov[110], K. Shaw[155], S. M. Shaw[99], A. Shcherbakova[137], Y. Shen[127], N. Sherafati[34], A. D. Sherman[25], P. Sherwood[93], L. Shi[157,as], S. Shimizu[80], C. O. Shimmin[182], Y. Shimogama[178], M. Shimojima[115], I. P. J. Shipsey[134], S. Shirabe[86], M. Shiyakova[78,ab], J. Shlomi[179], A. Shmeleva[109], M. J. Shochet[37], S. Shojaii[103], D. R. Shope[127], S. Shrestha[125], E. Shulga[111], P. Sicho[140], A. M. Sickles[172], P. E. Sidebo[153], E. Sideras Haddad[33c], O. Sidiropoulou[36], A. Sidoti[23b,23a], F. Siegert[47], Dj. Sijacki[16], J. Silva[139a], M. Silva Jr.[180], M. V. Silva Oliveira[79a], S. B. Silverstein[44a], S. Simion[131], E. Simioni[98], M. Simon[98], R. Simoniello[98], P. Sinervo[166], N. B. Sinev[130], M. Sioli[23b,23a], I. Siral[104], S. Yu. Sivoklokov[112], J. Sjölin[44a,44b], P. Skubic[127], M. Slawinska[83], K. Sliwa[169], R. Slovak[142], V. Smakhtin[179], B. H. Smart[5], J. Smiesko[28a], N. Smirnov[111], S. Yu. Smirnov[111], Y. Smirnov[111], L. N. Smirnova[112,t], O. Smirnova[95], J. W. Smith[52], M. Smizanska[88], K. Smolek[141], A. Smykiewicz[83], A. A. Snesarev[109], I. M. Snyder[130], S. Snyder[29], R. Sobie[175,ad], A. M. Soffa[170], A. Soffer[160], A. Søgaard[49], F. Sohns[52], G. Sokhrannyi[90], C. A. Solans Sanchez[36], E. Yu. Soldatov[111], U. Soldevila[173], A. A. Solodkov[122], A. Soloshenko[78], O. V. Solovyanov[122], V. Solovyev[137], P. Sommer[148], H. Son[169], W. Song[143], W. Y. Song[167b], A. Sopczak[141], F. Sopkova[28b], C. L. Sotiropoulou[70a,70b], S. Sottocornola[69a,69b], R. Soualah[65a,65c,h], A. M. Soukharev[121b,121a], D. South[45], S. Spagnolo[66a,66b], M. Spalla[114], M. Spangenberg[177], F. Spanò[92], D. Sperlich[19], T. M. Spieker[60a], R. Spighi[23b], G. Spigo[36], L. A. Spiller[103], D. P. Spiteri[56], M. Spousta[142], A. Stabile[67a,67b], B. L. Stamas[120], R. Stamen[60a], M. Stamenkovic[119], S. Stamm[19], E. Stanecka[83], R. W. Stanek[6], B. Stanislaus[134], M. M. Stanitzki[45], B. Stapf[119], E. A. Starchenko[122], G. H. Stark[145], J. Stark[57], S. H. Stark[40], P. Staroba[140], P. Starovoitov[60a], S. Stärz[102], R. Staszewski[83], M. Stegler[45], P. Steinberg[29], B. Stelzer[151], H. J. Stelzer[36], O. Stelzer-Chilton[167a], H. Stenzel[55], T. J. Stevenson[155], G. A. Stewart[36], M. C. Stockton[36], G. Stoicea[27b], P. Stolte[52], S. Stonjek[114], A. Straessner[47], J. Strandberg[153], S. Strandberg[44a,44b], M. Strauss[127], P. Strizenec[28b], R. Ströhmer[176], D. M. Strom[130], R. Stroynowski[42], A. Strubig[49], S. A. Stucci[29], B. Stugu[17], J. Stupak[127], N. A. Styles[45], D. Su[152], S. Suchek[60a], Y. Sugaya[132], V. V. Sulin[109], M. J. Sullivan[89], D. M. S. Sultan[53], S. Sultansoy[4c], T. Sumida[84], S. Sun[104], X. Sun[3], K. Suruliz[155], C. J. E. Suster[156], M. R. Sutton[155], S. Suzuki[80], M. Svatos[140], M. Swiatlowski[37], S. P. Swift[2], A. Sydorenko[98], I. Sykora[28a], M. Sykora[142], T. Sykora[142], D. Ta[98], K. Tackmann[45,z], J. Taenzer[160], A. Taffard[170], R. Tafirout[167a], E. Tahirovic[91], N. Taiblum[160], H. Takai[29], R. Takashima[85], K. Takeda[81], T. Takeshita[149], Y. Takubo[80], M. Talby[100], A. A. Talyshev[121b,121a], J. Tanaka[162], M. Tanaka[164], R. Tanaka[131], B. B. Tannenwald[125], S. Tapia Araya[172], S. Tapprogge[98], A. Tarek Abouelfadl Mohamed[135], S. Tarem[159], G. Tarna[27b,d], G. F. Tartarelli[67a], P. Tas[142], M. Tasevsky[140], T. Tashiro[84], E. Tassi[41b,41a], A. Tavares Delgado[139a,139b], Y. Tayalati[35e], A. J. Taylor[49], G. N. Taylor[103], P. T. E. Taylor[103], W. Taylor[167b], A. S. Tee[88], R. Teixeira De Lima[152], P. Teixeira-Dias[92], H. Ten Kate[36], J. J. Teoh[119], S. Terada[80], K. Terashi[162], J. Terron[97], S. Terzo[14], M. Testa[50], R. J. Teuscher[166,ad], S. J. Thais[182], T. Theveneaux-Pelzer[45], F. Thiele[40], D. W. Thomas[92], J. P. Thomas[21], A. S. Thompson[56], P. D. Thompson[21], L. A. Thomsen[182], E. Thomson[136], Y. Tian[39], R. E. Ticse Torres[52], V. O. Tikhomirov[109,ap], Yu. A. Tikhonov[121b,121a], S. Timoshenko[111], P. Tipton[182], S. Tisserant[100], K. Todome[164], S. Todorova-Nova[5], S. Todt[47], J. Tojo[86], S. Tokár[28a], K. Tokushuku[80], E. Tolley[125], K. G. Tomiwa[33c], M. Tomoto[116], L. Tompkins[152,q], K. Toms[117], B. Tong[58], P. Tornambe[51], E. Torrence[130], H. Torres[47], E. Torró Pastor[147], C. Tosciri[134], J. Toth[100,ac], D. R. Tovey[148], C. J. Treado[123], T. Trefzger[176], F. Tresoldi[155], A. Tricoli[29], I. M. Trigger[167a], S. Trincaz-Duvoid[135], W. Trischuk[166], B. Trocmé[57], A. Trofymov[131], C. Troncon[67a], M. Trovatelli[175], F. Trovato[155], L. Truong[33b], M. Trzebinski[83], A. Trzupek[83], F. Tsai[45], J.C-L. Tseng[134], P. V. Tsiareshka[106,aj], A. Tsirigotis[161], N. Tsirintanis[9], V. Tsiskaridze[154], E. G. Tskhadadze[158a], I. I. Tsukerman[110], V. Tsulaia[18], S. Tsuno[80], D. Tsybychev[154], Y. Tu[62b], A. Tudorache[27b], V. Tudorache[27b], T. T. Tulbure[27a], A. N. Tuna[58], S. Turchikhin[78], D. Turgeman[179], I. Turk Cakir[4b,u], R. J. Turner[21], R. T. Turra[67a], P. M. Tuts[39], S Tzamarias[161], E. Tzovara[98], G. Ucchielli[46], I. Ueda[80], M. Ughetto[44a,44b], F. Ukegawa[168], G. Unal[36], A. Undrus[29], G. Unel[170], F. C. Ungaro[103], Y. Unno[80], K. Uno[162], J. Urban[28b], P. Urquijo[103], G. Usai[8], J. Usui[80], L. Vacavant[100], V. Vacek[141], B. Vachon[102], K. O. H. Vadla[133], A. Vaidya[93], C. Valderanis[113], E. Valdes Santurio[44a,44b], M. Valente[53], S. Valentinetti[23b,23a], A. Valero[173], L. Valéry[45], R. A. Vallance[21], A. Vallier[5], J. A. Valls Ferrer[173], T. R. Van Daalen[14], P. Van Gemmeren[6], I. Van Vulpen[119], M. Vanadia[72a,72b], W. Vandelli[36], A. Vaniachine[165], R. Vari[71a], E. W. Varnes[7], C. Varni[54b,54a], T. Varol[42], D. Varouchas[131], K. E. Varvell[156], G. A. Vasquez[146b], J. G. Vasquez[182], F. Vazeille[38], D. Vazquez Furelos[14], T. Vazquez Schroeder[36], J. Veatch[52], V. Vecchio[73a,73b], L. M. Veloce[166], F. Veloso[139a,139c], S. Veneziano[71a], A. Ventura[66a,66b], N. Venturi[36], A. Verbytskyi[114], V. Vercesi[69a], M. Verducci[73a,73b], C. M. Vergel Infante[77], C. Vergis[24], W. Verkerke[119], A. T. Vermeulen[119], J. C. Vermeulen[119], M. C. Vetterli[151,aw], N. Viaux Maira[146b], M. Vicente Barreto Pinto[53], I. Vichou[172,*], T. Vickey[148], O. E. Vickey Boeriu[148], G. H. A. Viehhauser[134], L. Vigani[134], M. Villa[23b,23a], M. Villaplana Perez[67a,67b], E. Vilucchi[50], M. G. Vincter[34], V. B. Vinogradov[78], A. Vishwakarma[45], C. Vittori[23b,23a], I. Vivarelli[155], M. Vogel[181], P. Vokac[141], G. Volpi[14], S. E. von Buddenbrock[33c], E. Von Toerne[24],

V. Vorobel[142], K. Vorobev[111], M. Vos[173], J. H. Vossebeld[89], N. Vranjes[16], M. Vranjes Milosavljevic[16], V. Vrba[141], M. Vreeswijk[119], T. Šfiligoj[90], R. Vuillermet[36], I. Vukotic[37], T. Ženiš[28a], L. Živković[16], P. Wagner[24], W. Wagner[181], J. Wagner-Kuhr[113], H. Wahlberg[87], S. Wahrmund[47], K. Wakamiya[81], V. M. Walbrecht[114], J. Walder[88], R. Walker[113], S. D. Walker[92], W. Walkowiak[150], V. Wallangen[44a,44b], A. M. Wang[58], C. Wang[59b], F. Wang[180], H. Wang[18], H. Wang[3], J. Wang[156], J. Wang[60b], P. Wang[42], Q. Wang[127], R.-J. Wang[135], R. Wang[59a], R. Wang[6], S. M. Wang[157], W. T. Wang[59a], W. Wang[15c,ae], W. X. Wang[59a,ae], Y. Wang[59a,am], Z. Wang[59c], C. Wanotayaroj[45], A. Warburton[102], C. P. Ward[32], D. R. Wardrope[93], A. Washbrook[49], A. T. Watson[21], M. F. Watson[21], G. Watts[147], B. M. Waugh[93], A. F. Webb[11], S. Webb[98], C. Weber[182], M. S. Weber[20], S. A. Weber[34], S. M. Weber[60a], A. R. Weidberg[134], J. Weingarten[46], M. Weirich[98], C. Weiser[51], P. S. Wells[36], T. Wenaus[29], T. Wengler[36], S. Wenig[36], N. Wermes[24], M. D. Werner[77], P. Werner[36], M. Wessels[60a], T. D. Weston[20], K. Whalen[130], N. L. Whallon[147], A. M. Wharton[88], A. S. White[104], A. White[8], M. J. White[1], R. White[146b], D. Whiteson[170], B. W. Whitmore[88], F. J. Wickens[143], W. Wiedenmann[180], M. Wielers[143], C. Wiglesworth[40], L. A. M. Wiik-Fuchs[51], F. Wilk[99], H. G. Wilkens[36], L. J. Wilkins[92], H. H. Williams[136], S. Williams[32], C. Willis[105], S. Willocq[101], J. A. Wilson[21], I. Wingerter-Seez[5], E. Winkels[155], F. Winklmeier[130], O. J. Winston[155], B. T. Winter[51], M. Wittgen[152], M. Wobisch[94], A. Wolf[98], T. M. H. Wolf[119], R. Wolff[100], J. Wollrath[51], M. W. Wolter[83], H. Wolters[139a,139c], V. W. S. Wong[174], N. L. Woods[145], S. D. Worm[21], B. K. Wosiek[83], K. W. Woźniak[83], K. Wraight[56], S. L. Wu[180], X. Wu[53], Y. Wu[59a], T. R. Wyatt[99], B. M. Wynne[49], S. Xella[40], Z. Xi[104], L. Xia[177], D. Xu[15a], H. Xu[59a,d], L. Xu[29], T. Xu[144], W. Xu[104], Z. Xu[152], B. Yabsley[156], S. Yacoob[33a], K. Yajima[132], D. P. Yallup[93], D. Yamaguchi[164], Y. Yamaguchi[164], A. Yamamoto[80], T. Yamanaka[162], F. Yamane[81], M. Yamatani[162], T. Yamazaki[162], Y. Yamazaki[81], Z. Yan[25], H. J. Yang[59c,59d], H. T. Yang[18], S. Yang[76], Y. Yang[162], Z. Yang[17], W-M. Yao[18], Y. C. Yap[45], Y. Yasu[80], E. Yatsenko[59c,59d], J. Ye[42], S. Ye[29], I. Yeletskikh[78], E. Yigitbasi[25], E. Yildirim[98], K. Yorita[178], K. Yoshihara[136], C. J. S. Young[36], C. Young[152], J. Yu[77], X. Yue[60a], S. P. Y. Yuen[24], B. Zabinski[83], G. Zacharis[10], E. Zaffaroni[53], R. Zaidan[14], A. M. Zaitsev[122,ao], T. Zakareishvili[158b], N. Zakharchuk[34], S. Zambito[58], D. Zanzi[36], D. R. Zaripovas[56], S. V. Zeißner[46], C. Zeitnitz[181], G. Zemaityte[134], J. C. Zeng[172], O. Zenin[122], D. Zerwas[131], M. Zgubič[134], D. F. Zhang[15b], F. Zhang[180], G. Zhang[59a], G. Zhang[15b], H. Zhang[15c], J. Zhang[6], L. Zhang[15c], L. Zhang[59a], M. Zhang[172], R. Zhang[59a], R. Zhang[24], X. Zhang[59b], Y. Zhang[15a,15d], Z. Zhang[62a], Z. Zhang[131], P. Zhao[48], Y. Zhao[59b], Z. Zhao[59a], A. Zhemchugov[78], Z. Zheng[104], D. Zhong[172], B. Zhou[104], C. Zhou[180], M. S. Zhou[15a,15d], M. Zhou[154], N. Zhou[59c], Y. Zhou[7], C. G. Zhu[59b], H. L. Zhu[59a], H. Zhu[15a], J. Zhu[104], Y. Zhu[59a], X. Zhuang[15a], K. Zhukov[109], V. Zhulanov[121b,121a], A. Zibell[176], D. Zieminska[64], N. I. Zimine[78], S. Zimmermann[51], Z. Zinonos[114], M. Ziolkowski[150], G. Zobernig[180], A. Zoccoli[23b,23a], K. Zoch[52], T. G. Zorbas[148], R. Zou[37], L. Zwalinski[36]

[1] Department of Physics, University of Adelaide, Adelaide, Australia
[2] Physics Department, SUNY Albany, Albany, NY, USA
[3] Department of Physics, University of Alberta, Edmonton, AB, Canada
[4] [(a)]Department of Physics, Ankara University, Ankara, Turkey; [(b)]Istanbul Aydin University, Istanbul, Turkey; [(c)]Division of Physics, TOBB University of Economics and Technology, Ankara, Turkey
[5] LAPP, Université Grenoble Alpes, Université Savoie Mont Blanc, CNRS/IN2P3, Annecy, France
[6] High Energy Physics Division, Argonne National Laboratory, Argonne, IL, USA
[7] Department of Physics, University of Arizona, Tucson, AZ, USA
[8] Department of Physics, University of Texas at Arlington, Arlington, TX, USA
[9] Physics Department, National and Kapodistrian University of Athens, Athens, Greece
[10] Physics Department, National Technical University of Athens, Zografou, Greece
[11] Department of Physics, University of Texas at Austin, Austin, TX, USA
[12] [(a)]Bahcesehir University, Faculty of Engineering and Natural Sciences, Istanbul, Turkey; [(b)]Istanbul Bilgi University, Faculty of Engineering and Natural Sciences, Istanbul, Turkey; [(c)]Department of Physics, Bogazici University, Istanbul, Turkey; [(d)]Department of Physics Engineering, Gaziantep University, Gaziantep, Turkey
[13] Institute of Physics, Azerbaijan Academy of Sciences, Baku, Azerbaijan
[14] Institut de Física d'Altes Energies (IFAE), Barcelona Institute of Science and Technology, Barcelona, Spain
[15] [(a)]Institute of High Energy Physics, Chinese Academy of Sciences, Beijing, China; [(b)]Physics Department, Tsinghua University, Beijing, China; [(c)]Department of Physics, Nanjing University, Nanjing, China; [(d)]University of Chinese Academy of Science (UCAS), Beijing, China
[16] Institute of Physics, University of Belgrade, Belgrade, Serbia
[17] Department for Physics and Technology, University of Bergen, Bergen, Norway
[18] Physics Division, Lawrence Berkeley National Laboratory and University of California, Berkeley, CA, USA

[19] Institut für Physik, Humboldt Universität zu Berlin, Berlin, Germany
[20] Albert Einstein Center for Fundamental Physics and Laboratory for High Energy Physics, University of Bern, Bern, Switzerland
[21] School of Physics and Astronomy, University of Birmingham, Birmingham, UK
[22] Facultad de Ciencias y Centro de Investigaciónes, Universidad Antonio Nariño, Bogota, Colombia
[23] [(a)]Dipartimento di Fisica, INFN Bologna and Università di Bologna, Bologna, Italy; [(b)]INFN Sezione di Bologna, Bologna, Italy
[24] Physikalisches Institut, Universität Bonn, Bonn, Germany
[25] Department of Physics, Boston University, Boston, MA, USA
[26] Department of Physics, Brandeis University, Waltham, MA, USA
[27] [(a)]Transilvania University of Brasov, Brasov, Romania; [(b)]Horia Hulubei National Institute of Physics and Nuclear Engineering, Bucharest, Romania; [(c)]Department of Physics, Alexandru Ioan Cuza University of Iasi, Iasi, Romania ; [(d)]National Institute for Research and Development of Isotopic and Molecular Technologies, Physics Department, Cluj-Napoca, Romania; [(e)]University Politehnica Bucharest, Bucharest, Romania; [(f)]West University in Timisoara, Timisoara, Romania
[28] [(a)]Faculty of Mathematics, Physics and Informatics, Comenius University, Bratislava, Slovakia; [(b)]Department of Subnuclear Physics, Institute of Experimental Physics of the Slovak Academy of Sciences, Kosice, Slovak Republic
[29] Physics Department, Brookhaven National Laboratory, Upton, NY, USA
[30] Departamento de Física, Universidad de Buenos Aires, Buenos Aires, Argentina
[31] California State University, CA, USA
[32] Cavendish Laboratory, University of Cambridge, Cambridge, UK
[33] [(a)]Department of Physics, University of Cape Town, Cape Town, South Africa; [(b)]Department of Mechanical Engineering Science, University of Johannesburg, Johannesburg, South Africa; [(c)]School of Physics, University of the Witwatersrand, Johannesburg, South Africa
[34] Department of Physics, Carleton University, Ottawa, ON, Canada
[35] [(a)]Faculté des Sciences Ain Chock, Réseau Universitaire de Physique des Hautes Energies-Université Hassan II, Casablanca, Morocco; [(b)]Faculté des Sciences, Université Ibn-Tofail, Kénitra, Morocco; [(c)]Faculté des Sciences Semlalia, Université Cadi Ayyad, LPHEA-Marrakech, Marrakesh, Morocco; [(d)]Faculté des Sciences, Université Mohamed Premier and LPTPM, Oujda, Morocco; [(e)]Faculté des sciences, Université Mohammed V, Rabat, Morocco
[36] CERN, Geneva, Switzerland
[37] Enrico Fermi Institute, University of Chicago, Chicago, IL, USA
[38] LPC, Université Clermont Auvergne, CNRS/IN2P3, Clermont-Ferrand, France
[39] Nevis Laboratory, Columbia University, Irvington, NY, USA
[40] Niels Bohr Institute, University of Copenhagen, Copenhagen, Denmark
[41] [(a)]Dipartimento di Fisica, Università della Calabria, Rende, Italy; [(b)]INFN Gruppo Collegato di Cosenza, Laboratori Nazionali di Frascati, Italy
[42] Physics Department, Southern Methodist University, Dallas, TX, USA
[43] Physics Department, University of Texas at Dallas, Richardson, TX, USA
[44] [(a)]Department of Physics, Stockholm University, Stockholm, Sweden; [(b)]Oskar Klein Centre, Stockholm, Sweden
[45] Deutsches Elektronen-Synchrotron DESY, Hamburg and Zeuthen, Germany
[46] Lehrstuhl für Experimentelle Physik IV, Technische Universität Dortmund, Dortmund, Germany
[47] Institut für Kern- und Teilchenphysik, Technische Universität Dresden, Dresden, Germany
[48] Department of Physics, Duke University, Durham, NC, USA
[49] SUPA - School of Physics and Astronomy, University of Edinburgh, Edinburgh, UK
[50] INFN e Laboratori Nazionali di Frascati, Frascati, Italy
[51] Physikalisches Institut, Albert-Ludwigs-Universität Freiburg, Freiburg, Germany
[52] II. Physikalisches Institut, Georg-August-Universität Göttingen, Göttingen, Germany
[53] Département de Physique Nucléaire et Corpusculaire, Université de Genève, Genève, Switzerland
[54] [(a)]Dipartimento di Fisica, Università di Genova, Genova, Italy; [(b)]INFN Sezione di Genova, Genoa, Italy
[55] II. Physikalisches Institut, Justus-Liebig-Universität Giessen, Giessen, Germany
[56] SUPA - School of Physics and Astronomy, University of Glasgow, Glasgow, UK
[57] LPSC, Université Grenoble Alpes, CNRS/IN2P3, Grenoble INP, Grenoble, France
[58] Laboratory for Particle Physics and Cosmology, Harvard University, Cambridge, MA, USA

[59] [(a)]Department of Modern Physics and State Key Laboratory of Particle Detection and Electronics, University of Science and Technology of China, Hefei, China; [(b)]Institute of Frontier and Interdisciplinary Science and Key Laboratory of Particle Physics and Particle Irradiation (MOE), Shandong University, Qingdao, China; [(c)]School of Physics and Astronomy, Shanghai Jiao Tong University, KLPPAC-MoE, SKLPPC, Shanghai, China; [(d)]Tsung-Dao Lee Institute, Shanghai, China
[60] [(a)]Kirchhoff-Institut für Physik, Ruprecht-Karls-Universität Heidelberg, Heidelberg, Germany; [(b)]Physikalisches Institut, Ruprecht-Karls-Universität Heidelberg, Heidelberg, Germany
[61] Faculty of Applied Information Science, Hiroshima Institute of Technology, Hiroshima, Japan
[62] [(a)]Department of Physics, , Chinese University of Hong Kong, Shatin, N.T., Hong Kong, China; [(b)]Department of Physics, University of Hong Kong, Hong Kong, China; [(c)]Department of Physics and Institute for Advanced Study, Hong Kong University of Science and Technology, Clear Water Bay, Kowloon, Hong Kong, China
[63] Department of Physics, National Tsing Hua University, Hsinchu, Taiwan
[64] Department of Physics, Indiana University, Bloomington, IN, USA
[65] [(a)]INFN Gruppo Collegato di Udine, Sezione di Trieste, Udine, Italy; [(b)]ICTP, Trieste, Italy; [(c)]Dipartimento Politecnico di Ingegneria e Architettura, Università di Udine, Udine, Italy
[66] [(a)]INFN Sezione di Lecce, Lecce, Italy; [(b)]Dipartimento di Matematica e Fisica, Università del Salento, Lecce, Italy
[67] [(a)]INFN Sezione di Milano, Milan, Italy; [(b)]Dipartimento di Fisica, Università di Milano, Milano, Italy
[68] [(a)]INFN Sezione di Napoli, Naples, Italy; [(b)]Dipartimento di Fisica, Università di Napoli, Napoli, Italy
[69] [(a)]INFN Sezione di Pavia, Pavia, Italy; [(b)]Dipartimento di Fisica, Università di Pavia, Pavia, Italy
[70] [(a)]INFN Sezione di Pisa, Pisa, Italy; [(b)]Dipartimento di Fisica E. Fermi, Università di Pisa, Pisa, Italy
[71] [(a)]INFN Sezione di Roma, Rome, Italy; [(b)]Dipartimento di Fisica, Sapienza Università di Roma, Roma, Italy
[72] [(a)]INFN Sezione di Roma Tor Vergata, Rome, Italy; [(b)]Dipartimento di Fisica, Università di Roma Tor Vergata, Roma, Italy
[73] [(a)]INFN Sezione di Roma Tre, Rome, Italy; [(b)]Dipartimento di Matematica e Fisica, Università Roma Tre, Roma, Italy
[74] [(a)]INFN-TIFPA, Povo, Italy; [(b)]Università degli Studi di Trento, Trento, Italy
[75] Institut für Astro- und Teilchenphysik, Leopold-Franzens-Universität, Innsbruck, Austria
[76] University of Iowa, Iowa City, IA, USA
[77] Department of Physics and Astronomy, Iowa State University, Ames, IA, USA
[78] Joint Institute for Nuclear Research, Dubna, Russia
[79] [(a)]Departamento de Engenharia Elétrica, Universidade Federal de Juiz de Fora (UFJF), Juiz de Fora, Brazil; [(b)]Universidade Federal do Rio De Janeiro COPPE/EE/IF, Rio de Janeiro, Brazil; [(c)]Universidade Federal de São João del Rei (UFSJ), São João del Rei, Brazil; [(d)]Instituto de Física, Universidade de São Paulo, São Paulo, Brazil
[80] KEK, High Energy Accelerator Research Organization, Tsukuba, Japan
[81] Graduate School of Science, Kobe University, Kobe, Japan
[82] [(a)]AGH University of Science and Technology, Faculty of Physics and Applied Computer Science, Kraków, Poland; [(b)]Marian Smoluchowski Institute of Physics, Jagiellonian University, Krakow, Poland
[83] Institute of Nuclear Physics Polish Academy of Sciences, Krakow, Poland
[84] Faculty of Science, Kyoto University, Kyoto, Japan
[85] Kyoto University of Education, Kyoto, Japan
[86] Research Center for Advanced Particle Physics and Department of Physics, Kyushu University, Fukuoka , Japan
[87] Instituto de Física La Plata, Universidad Nacional de La Plata and CONICET, La Plata, Argentina
[88] Physics Department, Lancaster University, Lancaster, UK
[89] Oliver Lodge Laboratory, University of Liverpool, Liverpool, UK
[90] Department of Experimental Particle Physics, Jožef Stefan Institute and Department of Physics, University of Ljubljana, Ljubljana, Slovenia
[91] School of Physics and Astronomy, Queen Mary University of London, London, UK
[92] Department of Physics, Royal Holloway University of London, Egham, UK
[93] Department of Physics and Astronomy, University College London, London, UK
[94] Louisiana Tech University, Ruston, LA, USA
[95] Fysiska institutionen, Lunds universitet, Lund, Sweden
[96] Centre de Calcul de l'Institut National de Physique Nucléaire et de Physique des Particules (IN2P3), Villeurbanne, France
[97] Departamento de Física Teorica C-15 and CIAFF, Universidad Autónoma de Madrid, Madrid, Spain

[98] Institut für Physik, Universität Mainz, Mainz, Germany
[99] School of Physics and Astronomy, University of Manchester, Manchester, UK
[100] CPPM, Aix-Marseille Université, CNRS/IN2P3, Marseille, France
[101] Department of Physics, University of Massachusetts, Amherst, MA, USA
[102] Department of Physics, McGill University, Montreal, QC, Canada
[103] School of Physics, University of Melbourne, Victoria, Australia
[104] Department of Physics, University of Michigan, Ann Arbor, MI, USA
[105] Department of Physics and Astronomy, Michigan State University, East Lansing, MI, USA
[106] B.I. Stepanov Institute of Physics, National Academy of Sciences of Belarus, Minsk, Belarus
[107] Research Institute for Nuclear Problems of Byelorussian State University, Minsk, Belarus
[108] Group of Particle Physics, University of Montreal, Montreal, QC, Canada
[109] P.N. Lebedev Physical Institute of the Russian Academy of Sciences, Moscow, Russia
[110] Institute for Theoretical and Experimental Physics of the National Research Centre Kurchatov Institute, Moscow, Russia
[111] National Research Nuclear University MEPhI, Moscow, Russia
[112] D.V. Skobeltsyn Institute of Nuclear Physics, M.V. Lomonosov Moscow State University, Moscow, Russia
[113] Fakultät für Physik, Ludwig-Maximilians-Universität München, München, Germany
[114] Max-Planck-Institut für Physik (Werner-Heisenberg-Institut), München, Germany
[115] Nagasaki Institute of Applied Science, Nagasaki, Japan
[116] Graduate School of Science and Kobayashi-Maskawa Institute, Nagoya University, Nagoya, Japan
[117] Department of Physics and Astronomy, University of New Mexico, Albuquerque, NM, USA
[118] Institute for Mathematics, Astrophysics and Particle Physics, Radboud University Nijmegen/Nikhef, Nijmegen, Netherlands
[119] Nikhef National Institute for Subatomic Physics and University of Amsterdam, Amsterdam, Netherlands
[120] Department of Physics, Northern Illinois University, DeKalb, IL, USA
[121] [(a)]Budker Institute of Nuclear Physics and NSU, SB RAS, Novosibirsk, Russia; [(b)]Novosibirsk State University Novosibirsk, Novosibirsk, Russia
[122] Institute for High Energy Physics of the National Research Centre Kurchatov Institute, Protvino, Russia
[123] Department of Physics, New York University, New York, NY, USA
[124] Ochanomizu University, Otsuka, Bunkyo-ku, Tokyo, Japan
[125] Ohio State University, Columbus, OH, USA
[126] Faculty of Science, Okayama University, Okayama, Japan
[127] Homer L. Dodge Department of Physics and Astronomy, University of Oklahoma, Norman, OK, USA
[128] Department of Physics, Oklahoma State University, Stillwater, OK, USA
[129] Palacký University, RCPTM, Joint Laboratory of Optics, Olomouc, Czech Republic
[130] Center for High Energy Physics, University of Oregon, Eugene, OR, USA
[131] LAL, Université Paris-Sud, CNRS/IN2P3, Université Paris-Saclay, Orsay, France
[132] Graduate School of Science, Osaka University, Osaka, Japan
[133] Department of Physics, University of Oslo, Oslo, Norway
[134] Department of Physics, Oxford University, Oxford, UK
[135] LPNHE, Sorbonne Université, Paris Diderot Sorbonne Paris Cité, CNRS/IN2P3, Paris, France
[136] Department of Physics, University of Pennsylvania, Philadelphia, PA, USA
[137] Konstantinov Nuclear Physics Institute of National Research Centre "Kurchatov Institute", PNPI, St. Petersburg, Russia
[138] Department of Physics and Astronomy, University of Pittsburgh, Pittsburgh, PA, USA
[139] [(a)]Laboratório de Instrumentação e Física Experimental de Partículas-LIP, Lisbon, Portugal; [(b)]Departamento de Física, Faculdade de Ciências, Universidade de Lisboa, Lisbon, Portugal; [(c)]Departamento de Física, Universidade de Coimbra, Coimbra, Portugal; [(d)]Centro de Física Nuclear da Universidade de Lisboa, Lisbon, Portugal; [(e)]Departamento de Física, Universidade do Minho, Braga, Portugal; [(f)]Universidad de Granada, Granada, Spain; [(g)]Dep Física and CEFITEC of Faculdade de Ciências e Tecnologia, Universidade Nova de Lisboa, Caparica, Portugal
[140] Institute of Physics of the Czech Academy of Sciences, Prague, Czech Republic
[141] Czech Technical University in Prague, Prague, Czech Republic
[142] Charles University, Faculty of Mathematics and Physics, Prague, Czech Republic
[143] Particle Physics Department, Rutherford Appleton Laboratory, Didcot, UK
[144] IRFU, CEA, Université Paris-Saclay, Gif-sur-Yvette, France

[145] Santa Cruz Institute for Particle Physics, University of California Santa Cruz, Santa Cruz, CA, USA
[146] [(a)]Departamento de Física, Pontificia Universidad Católica de Chile, Santiago, Chile; [(b)]Departamento de Física, Universidad Técnica Federico Santa María, Valparaíso, Chile
[147] Department of Physics, University of Washington, Seattle, WA, USA
[148] Department of Physics and Astronomy, University of Sheffield, Sheffield, UK
[149] Department of Physics, Shinshu University, Nagano, Japan
[150] Department Physik, Universität Siegen, Siegen, Germany
[151] Department of Physics, Simon Fraser University, Burnaby, BC, Canada
[152] SLAC National Accelerator Laboratory, Stanford, CA, USA
[153] Physics Department, Royal Institute of Technology, Stockholm, Sweden
[154] Departments of Physics and Astronomy, Stony Brook University, Stony Brook, NY, USA
[155] Department of Physics and Astronomy, University of Sussex, Brighton, UK
[156] School of Physics, University of Sydney, Sydney, Australia
[157] Institute of Physics, Academia Sinica, Taipei, Taiwan
[158] [(a)]E. Andronikashvili Institute of Physics, Iv. Javakhishvili Tbilisi State University, Tbilisi, Georgia; [(b)]High Energy Physics Institute, Tbilisi State University, Tbilisi, Georgia
[159] Department of Physics, Technion, Israel Institute of Technology, Haifa, Israel
[160] Raymond and Beverly Sackler School of Physics and Astronomy, Tel Aviv University, Tel Aviv, Israel
[161] Department of Physics, Aristotle University of Thessaloniki, Thessaloniki, Greece
[162] International Center for Elementary Particle Physics and Department of Physics, University of Tokyo, Tokyo, Japan
[163] Graduate School of Science and Technology, Tokyo Metropolitan University, Tokyo, Japan
[164] Department of Physics, Tokyo Institute of Technology, Tokyo, Japan
[165] Tomsk State University, Tomsk, Russia
[166] Department of Physics, University of Toronto, Toronto, ON, Canada
[167] [(a)]TRIUMF, Vancouver, BC, Canada; [(b)]Department of Physics and Astronomy, York University, Toronto, ON, Canada
[168] Division of Physics and Tomonaga Center for the History of the Universe, Faculty of Pure and Applied Sciences, University of Tsukuba, Tsukuba, Japan
[169] Department of Physics and Astronomy, Tufts University, Medford, MA, USA
[170] Department of Physics and Astronomy, University of California Irvine, Irvine, CA, USA
[171] Department of Physics and Astronomy, University of Uppsala, Uppsala, Sweden
[172] Department of Physics, University of Illinois, Urbana, IL, USA
[173] Instituto de Física Corpuscular (IFIC), Centro Mixto Universidad de Valencia - CSIC, Valencia, Spain
[174] Department of Physics, University of British Columbia, Vancouver, BC, Canada
[175] Department of Physics and Astronomy, University of Victoria, Victoria, BC, Canada
[176] Fakultät für Physik und Astronomie, Julius-Maximilians-Universität Würzburg, Würzburg, Germany
[177] Department of Physics, University of Warwick, Coventry, UK
[178] Waseda University, Tokyo, Japan
[179] Department of Particle Physics, Weizmann Institute of Science, Rehovot, Israel
[180] Department of Physics, University of Wisconsin, Madison, WI, USA
[181] Fakultät für Mathematik und Naturwissenschaften, Fachgruppe Physik, Bergische Universität Wuppertal, Wuppertal, Germany
[182] Department of Physics, Yale University, New Haven, CT, USA
[183] Yerevan Physics Institute, Yerevan, Armenia

[a] Also at Borough of Manhattan Community College, City University of New York, New York, NY, USA
[b] Also at Centre for High Performance Computing, CSIR Campus, Rosebank, Cape Town;, South Africa
[c] Also at CERN, Geneva, Switzerland
[d] Also at CPPM, Aix-Marseille Université, CNRS/IN2P3, Marseille, France
[e] Also at Département de Physique Nucléaire et Corpusculaire, Université de Genève, Genève, Switzerland
[f] Also at Departament de Fisica de la Universitat Autonoma de Barcelona, Barcelona, Spain
[g] Also at Departamento de Física, Instituto Superior Técnico, Universidade de Lisboa, Lisboa, Portugal
[h] Also at Department of Applied Physics and Astronomy, University of Sharjah, Sharjah, United Arab Emirates
[i] Also at Department of Financial and Management Engineering, University of the Aegean, Chios, Greece

[j] Also at Department of Physics and Astronomy, University of Louisville, Louisville, KY, USA
[k] Also at Department of Physics and Astronomy, University of Sheffield, Sheffield, UK
[l] Also at Department of Physics, California State University, East Bay, USA
[m] Also at Department of Physics, California State University, Fresno, USA
[n] Also at Department of Physics, California State University, Sacramento, USA
[o] Also at Department of Physics, King's College London, London, UK
[p] Also at Department of Physics, St. Petersburg State Polytechnical University, St. Petersburg, Russia
[q] Also at Department of Physics, Stanford University, Stanford CA, USA
[r] Also at Department of Physics, University of Fribourg, Fribourg, Switzerland
[s] Also at Department of Physics, University of Michigan, Ann Arbor MI, USA
[t] Also at Faculty of Physics, M.V. Lomonosov Moscow State University, Moscow, Russia
[u] Also at Giresun University, Faculty of Engineering, Giresun, Turkey
[v] Also at Graduate School of Science, Osaka University, Osaka, Japan
[w] Also at Hellenic Open University, Patras, Greece
[x] Also at Horia Hulubei National Institute of Physics and Nuclear Engineering, Bucharest, Romania
[y] Also at Institucio Catalana de Recerca i Estudis Avancats, ICREA, Barcelona, Spain
[z] Also at Institut für Experimentalphysik, Universität Hamburg, Hamburg, Germany
[aa] Also at Institute for Mathematics, Astrophysics and Particle Physics, Radboud University Nijmegen/Nikhef, Nijmegen, The Netherlands
[ab] Also at Institute for Nuclear Research and Nuclear Energy (INRNE) of the Bulgarian Academy of Sciences, Sofia, Bulgaria
[ac] Also at Institute for Particle and Nuclear Physics, Wigner Research Centre for Physics, Budapest, Hungary
[ad] Also at Institute of Particle Physics (IPP), Canada
[ae] Also at Institute of Physics, Academia Sinica, Taipei, Taiwan
[af] Also at Institute of Physics, Azerbaijan Academy of Sciences, Baku, Azerbaijan
[ag] Also at Institute of Theoretical Physics, Ilia State University, Tbilisi, Georgia
[ah] Also at Instituto de Fisica Teorica, IFT-UAM/CSIC, Madrid, Spain
[ai] Also at Istanbul University, Dept. of Physics, Istanbul, Turkey
[aj] Also at Joint Institute for Nuclear Research, Dubna, Russia
[ak] Also at LAL, Université Paris-Sud, CNRS/IN2P3, Université Paris-Saclay, Orsay, France
[al] Also at Louisiana Tech University, Ruston, LA, USA
[am] Also at LPNHE, Sorbonne Université, Paris Diderot Sorbonne Paris Cité, CNRS/IN2P3, Paris, France
[an] Also at Manhattan College, New York, NY, USA
[ao] Also at Moscow Institute of Physics and Technology State University, Dolgoprudny, Russia
[ap] Also at National Research Nuclear University MEPhI, Moscow, Russia
[aq] Also at Physics Department, An-Najah National University, Nablus, Palestine
[ar] Also at Physikalisches Institut, Albert-Ludwigs-Universität Freiburg, Freiburg, Germany
[as] Also at School of Physics, Sun Yat-sen University, Guangzhou, China
[at] Also at The City College of New York, New York, NY, USA
[au] Also at The Collaborative Innovation Center of Quantum Matter (CICQM), Beijing, China
[av] Also at Tomsk State University, Tomsk, and Moscow Institute of Physics and Technology State University, Dolgoprudny, Russia
[aw] Also at TRIUMF, Vancouver, BC, Canada
[ax] Also at Universidad de Granada, Granada (Spain), Spain
[ay] Also at Universita di Napoli Parthenope, Napoli, Italy
* Deceased